Submitted to **ADVANCED MATERIALS**

DNA Origami-Driven Lithography for Patterning on Gold Surfaces with Sub-10 Nanometer Resolution

By Isaac Gállego,* Brendan Manning, Joan Daniel Prades, Mònica Mir, Josep Samitier and *Ramon Eritja**

[*]   Dr I. Gállego, Dr B. Manning and Prof. Dr. R. Eritja
Institute for Advanced Chemistry of Catalonia (IQAC)
Networking Center in Bioengineering, Biomaterials and Nanomedicine (CIBER-BBN)
Spanish National Research Council (CSIC)
Barcelona 08034, Spain.
E-mail: (igallego@mrc-lmb.cam.ac.uk, recgma@cid.csic.es)
        Prof. J. D. Prades.
MIND-IN^{2}UB
Department of Engineering: Electronics
University of Barcelona
Barcelona 08028, Spain
        Dr. M Mir and Prof. Dr. J. Samitier
Institute for Bioengineering of Catalonia (IBEC)
Networking Center in Bioengineering, Biomaterials and Nanomedicine (CIBER-BBN)
Barcelona 08028, Spain

Current Address:
        Dr. Isaac Gállego
MRC Laboratory of Molecular Biology
Cambridge CB2 0HQ, UK

The programmability[1] and self-assembly properties of DNA provides means of precise organization of matter at the nanoscale.[2] DNA origami allows the folding of DNA into two-dimensional[3] and three-dimensional[4] structures, and has been used to organize biomolecules,[2b, e, 5] nanophotonic[2a, c, f, 6] and electronic[7] components with a resolution of 6 nm / pixel.[8] Two-dimensional DNA origami has been also used as a platform to organize other chemical[9] species that can then be placed on technologically relevant substrates.[2c, 10] Nevertheless, these approaches have only used the DNA nanostructure to hold the chemical species on the surface and, to the best of our knowledge, have never been utilized to immobilize nucleic acids patterns on surfaces with sub-10 nm resolution providing an enable

1

platform for potential applications such as multiplexed biochemical assays.[11] to the creation of metasurfaces[12] with potentially reconfigurable features.

Herein we report on the use of a two-dimensional DNA origami as a template to covalently attach DNA with a pre-programmed pattern on a surface (see **Scheme 1**). The method utilizes the incorporation of modified staple strands in programmed positions of the DNA origami (DNA origami stamp), acting as DNA ink. Once the DNA origami is immobilized on the surface, the modified staples can react with the surface creating a defined DNA pattern (**Stamping** step). The pattern can then be exposed upon denaturation of the DNA origami stamp (**Unmasking** step), allowing the non-bound staples to be rinsed off of the surface. As a proof-of-principle of this methodology, we have created a linear pattern of thiol-modified DNA ink on gold surfaces. The formation of the linear pattern was revealed by the successful formation of bead-on-a-string-like structures (here named "chains" for simplicity) composed of gold nanoparticles conjugated with thiol-oligonucleotides (OGNP) that are hybridized to the DNA ink pattern (**Development** step). The linear pattern provided a direct evidence of the stamping process and was chosen as a simple geometry that can be statistically analysed in our experimental setup. Montecarlo Simulations have been used for better understanding of our statistical results and to determine key elements governing the process that can be used for future optimization of pattern information transfer with DNA origami stamp methodology. Furthermore, we have studied the development of more complex patterns using Montecarlo Simulations.

We demonstrate that our approach can be employed to form DNA patterns with sub-10 nm resolution to flat gold surfaces, an unsolved goal to date. This methodology can thus be extended to other surfaces utilizing different covalent strategies.[10b, 13] Moreover, in combination with photolithography[8] and DNA origami lattice formation[14] methods, the process can be scale up to create micrometer scale patterns. The ability to program a pattern into a DNA origami frame and covalently transfer single DNA molecules further expands the

potential applications of DNA programmed materials,[15] while improving on the ability to recycle prescribed pattern and functionality, overcoming the bottlenecks associated with existent DNA-based methodologies for nanoscale patterning.[8,10]

Design and Assembly of DNA Origami Stamp. Tall rectangle DNA origami structures were assembled based on Rothemund's method.[3] To prepare DNA origami stamps with a thiolated DNA ink, 12 staple strands were replaced by the 5'-thiol-modified staples (ink staples; see Table S1). The thiol groups of the ink staples were protected with a disulfide group. This prevents interstrand dimerization, whilst the disulfide group can still react with the gold surface. The distance between 5'-thiols of DNA ink strands is of ~5.4 nm, according to the tall rectangle DNA origami design. Scheme 1a shows the programmed positions for the ink staples within the DNA origami to stamp a line on the gold surface. In our design we used two additional thiol-modified staples (anchor staples) to stabilize the interaction of the DNA origami with the gold surface.

A one-pot-reaction containing the M13mp18 scaffold (10 nM), the staple strands 10:1 (staple:scaffold molar ratio), and the 12 ink staples and the additional anchor staples (50:1 molar ratio) were mixed and thermally annealed as described previously.[3] The buffer used was 1X TAE, 12.5 mM Mg acetate pH 8. Fully assembled origami structures were purified from excess staple strands by using centrifugal filter devices. Correct formation of origami structures was confirmed by AFM on mica (Figure S1).

Stamping of a DNA Ink pattern on Gold Substrates. The first step of the **Stamping** process is to adsorb the DNA origami on the gold surfaces (Scheme 1b, step 1). A sample of purified DNA origami was spotted on a clean, preannealed gold surface and left to adsorb. Initial stable adsorption of the DNA origami is necessary for the formation of the thiol-gold bonding between the ink staples and the surface (see Supporting Information for details). On mica, a 12.5 mM of Mg^{2+} is required to mediate the adsorption of DNA origami structures. However, it has been described that on silica and diamond-like carbon an increased

concentration of divalent ions (100–125 mM Mg^{2+}) is required to promote the adhesion of

DNA origami.[8] Using the same approach we were able to adsorb the DNA origami stamps

on gold surfaces using 10 X TAE-Mg, containing 125 mM Mg^{2+}.

Surface plasmon resonance (SPR) analysis was used to monitor the **Stamping** process

in real time (**Figure 1**a), as SPR refractive angle shift is proportional to biomolecule

adsorption to a metal surface.[16] In our SPR set up, increased intensity correlates to DNA or

OGNP adhesion, and loss of intensity is due to desorption of the chemical species from the

surface. After addition of the DNA origami an increase of 3.29% of the intensity was

observed, indicating adsorption of the nanostructure on the gold surface. AFM imaging in

liquid confirmed the presence of rectangular–like structures over the gold surface with a size

in agreement with tall rectangle's design[3] (Figure 1b). The visualization of the DNA origami

stamps on gold surfaces is more difficult in comparison with the imaging on mica. The

weaker interaction of the DNA origami with gold surfaces and the roughness of gold,[10a] as

compared with mica, are the main factors affecting the image quality. However, the presence

of thiol-modified oligonucleotides within the DNA origami stamp provides additional anchor

points, and extra stability of the DNA structure to remain on the surface in comparison with

non-modified DNA origami (Figure S2); result that is in agreement with previous work in our

laboratory.[17]

The DNA origami stamp was then denatured in 0.05–0.1 M NaOH allowing the

removal of the DNA origami frame (i.e. the staple strands and the M13 scaffold). This

Unmasking step is necessary to expose the pattern of bound DNA ink molecules on the

surface (Scheme 1b, step 2). This step demonstrates the robustness of our method to DNA-

denaturing conditions; as compared with extant methods to place DNA origami on

surfaces,[10b] that can display chemical species,[10a] in which the pattern would be vulnerable

to any condition (i.e. temperature, pH, buffer salinity, solvent used) that can disrupt the

Watson-Crick base pairing and hamper further use of the programmable ability of DNA

nanostructure. SPR analysis confirmed reduction of 2.5 % of intensity in the refractive angle, indicating loss of the DNA origami frame (Figure 1a and S4).

Developing the DNA Pattern with Gold Nanoparticles. In order to characterize the transfer of the DNA ink pattern on the surface, we have used the hybridization of OGNPs as an example of reporter of the process. The **Developing** process was carried out in a two-step fashion (see Scheme 1b, step 3): i) The addition of a DNA bridge strand used to link the OGNP and the DNA ink; and ii) the attachment of the nanoparticle to the surface. The bridge sequences were hybridized directly to the OGNP (step 3) before the final hybridization of the OGNP on the surface to form the sandwich (4). During the Development we only used the bridge oligonucleotides complementary to the twelve DNA ink strands (see Table S3). The bridge oligonucleotide (30 bp long) is composed by two domains, one domain is complementary to 15 bp of each one of the DNA ink sequences, and the other domain contains a common sequence that is complementary to the oligonucleotide conjugated to the gold nanoparticles. The **Developing** process was followed by SPR and the OGNP chain formation was then characterized by scanning electron microscopy (SEM). For the SPR analysis the **Developing** procedure used was slightly different, here the bridge sequences were hybridized to the DNA ink pattern on the gold surface (Figure 2a) as opposed to the method used for the SEM visualisation, where the bridge sequence were hybridized directly onto the OGNP (Scheme 1). The protocol described in (Scheme 1) reduces excess of bridge oligonucleotide on the gold surfaces, minimizing undesired background.

The oligonucleotide-modified gold nanoparticles were prepared according to standard protocols described elsewhere.[18] Additionally, the resulting OGMPs were passivated with oligoethyleneglycol-thiol[19] to prevent non-specific binding to the gold surface (see Supporting Information).

Monitoring by SPR (Figure 1a and S4) showed hybridization of the bridge as indicated by an increase of 0.8 % of the refraction index intensity, while the hybridization of the OGNP

5

produced a larger increment of 19.3 % in the refractive index —the size, composition and structure of the OGNP are responsible for the greater change in the refractive index during SPR detection.[20] A control experiment in which the OGNP where added without the presence of the bridge sequence (Figure S4) showed SPR angle shift three times lower than in the presence of the DNA bridge, indicating sequence-specific hybridization of the OGNP with the DNA ink on the surface.

OGNP-chain formation on gold surfaces mediated by the DNA origami stamps was determined by SEM imaging. From now on, this procedure is designated as the "chain formation experiment" (CFE) as opposed to the "chain formation simulations" (CFS), in which chain formation is simulated *in silico* using Montecarlo Simulation methods (see Supporting Information for details). In both CFE and CFS procedures, the DNA ink pattern was **Developed** using OGNPs of 5 nm and 10 nm in diameter to investigate size-dependent effects on chain formation.

Analysis by SEM of the DNA origami stamping method revealed the formation of OGNP chains on the gold surfaces. **Figure 2**a shows a typical SEM field containing 10 nm OGNP chains of different size (red arrows heads). The yellow rectangles represent the DNA origami frame for comparison of size with OGNP chains. The insets in Figure 2b show selected chain images (see also Figures S6 and S7 for additional images) corresponding to each class of number of OGNP in a chain observed in CFE. Some of the chains do not contain straight OGNP alignments having zigzag-like shapes. This behavior was also observed in the CFS runs (Figure 3a and S8). In control experiments, we omitted the addition of the DNA origami stamp before **Unmasking** and **Development** steps; as a result no OGNP chains were formed (Figure S5).

DNA origami stamping method produced chains with a variable number of OGNP per chain. We then analyzed the distribution of the number of OGNPs per chain in both 5 nm and 10 nm nanoparticles (black circles in Figure 2c and e, respectively). Three OGNP in a chain

was considered as the minimum threshold for a DNA origami templated alignment of nanoparticles after determining the probability of forming spontaneous, non-templated chains in our experimental conditions (see Figure S5). These results indicated that the probability of spontaneously encountering a single OGNP was of 91.5% and the probability of finding 2-OGNP chains was still of 7.6%. In contrast, the spontaneous formation of 3-OGNP chains was a very seldom event occurring only in the 0.9% of cases. CFE statistics show a decay of the frequency upon increment of number of OGNP in a chain for both experiments, developed with 5 nm and 10 nm OGNP in diameter (Figure 2c and d). CFE analysis also showed that the apparent, statistically significant maximum number of particles in a chain was of 9 for the 5 nm OGNP and of 8 particles for the 10 nm OGNP.

The DNA origami design (Scheme 1) contained 12 DNA ink molecules that can be utilized to organize OGNP, each one containing DNA bridge sequences complementary to the 12 DNA ink, on the surface. This is a first step in the fabrication of more complex systems where-by each DNA ink strand is individually addressable if necessary, as compared to a system were each OGNP contains oligonucleotides complementary to a single or several (in close proximity) DNA ink sequences within the pattern. However, due to geometrical factors (i.e. DNA origami frame actual shape, steric restrictions due to OGNP size, and OGNP hybridization with more than one DNA ink spot, among others) the maximum apparent number of OGNP in a chain that a single DNA ink pattern can hold could be diminished. To test this hypothesis, we measured the geometric length of the chains observed in the CFE, end-to-end, for each chain class (i.e. chains containing a given number of OGNP). The analysis showed that there is a threshold number of nanoparticles within a chain at which the length plateaued at a value of about 70 nm for both 5 nm and 10 nm in diameter nanoparticles (Figure 2d and f). This length value corresponds to the width of the DNA origami frame, indicating that the maximum length of GNP chains corresponds to the length of the DNA origami used to stamp the pattern. This result was also confirmed by the CFS (Figure 2d and

f), corroborating that our geometric-based model recreates appropriately the chain formation process.

Subsequently, to identify the parameters that limit the apparent maximum number of OGNP in full-length chains and their yield, we utilized the *in silico* model of the DNA ink pattern and chain formation process. CFE results showed a decay in the frequency of longer chains, and a reduced number of full-length chains. In addition to purely geometrical arguments (see earlier in text, and Supporting Information), there are several factors that can lead to efficiency decrease of longer and full-length chains formation. Among them: i) DNA origami misfolding; ii) purity of thiol-oligonucleotides used as DNA ink; iii) the attachment efficiency of the DNA inks on the surface; and iv) the efficiency of particle hybridisation. In all, these factors will affect the total number and yield of active DNA ink within the pattern transferred to the surface and the OGNP binding to well-formed DNA ink; ultimately, creating regions in which the OGNP could not attach. To account for these effects, we defined the DNA ink yield (Y_{ink}) as the apparent fraction of well-formed DNA ink sites capable of hybridizing with the oligonucleotides covering the OGNP. This parameter effectively reduced the length and the full-length frequency of chains formed in our CFS runs (Figure 2c and e). The experimental analysis, CFE, corresponded to a Y_{ink} yield of 60% in the CFS data (Figure 2c and e) similar to previous reported data for a single anchorage point per particle on DNA origami structures.[21] Moreover, yield analysis using the CFS runs (Figure S9) showed that Y_{ink} yields over 90% will favor chains containing 8 OGNP for the 5 nm OGNP. On the other hand, the same high yields would favor chains containing 5-6 OGNP for 10 nm OGNP. Figure 3a shows examples of both types of alignment obtained in CFS runs. This result, un-anticipated from our initial CFE data, represents the main maximum chain lengths that could possibly be formed, according to our *in silico* model, with the nanoparticle's geometries used, in nearly ideal conditions. This result also points that increased yield on DNA ink printed on surface would dramatically increase the overall yield of chain formation. Among the possible

8

causes stated above, our CFS analysis indicates that increasing the yield of the DNA ink formation is an important factor. Therefore, the use of cyclic disulfides such as lipoic acid derivatives[13] reported to increase binding of oligonucleotides to gold surfaces combined with increased DNA ink that can bind per each OGNP,[21] would provide improved yields to our DNA origami stamp method for gold nanoparticle alignment. Figure S8 shows examples of OGNP of each class obtained in CFS runs. In addition to perfectly aligned chains of OGNP, CFS predicted zigzag arrangements similar to those observed in the CFE. The possibility to form close packed OGNP chains with zigzag-like shape, explains the diversity of lengths observed within each chain class and the plateau formation at a maximum length (approx. 70 nm, see Figure 2d and 2f); zigzag chains contain more particles than those that would nominally fit within the actual width of the full-length pattern (i.e. 70 nm), if straight alignment of OGNPs were formed. Intuitively, the use of bridge sequences might have facilitated the zigzag-like chain formation by increasing the length between gold surface and nanoparticle (maximum length of ~25 nm when extended), increasing the degree of freedom during chain formation in CFE. However, our CFS analysis pointed the same result based only on geometrical parameters of the OGNP, suggesting that reduction of the bridge length would not diminish the zigzag-like behavior in this system. Therefore, CFS corroborates the key role of DNA ink in the formation of the OGNP chain-like patterns, and provides insight into why different chain lengths emerge; a process mostly related to purely geometrical reasons combined with the yield of active DNA ink formation (see Supporting Information).

To further evaluate the universality of our DNA origami **Stamping** method to create larger and more complex patterns, we extended our linear pattern to a mesh of DNA ink corresponding to all possible DNA staple positions contained in the DNA origami stamp used in this work. Using this approach, we have created an *in silico* model of a rectangular mesh of DNA ink (Figure 3b) were we can perform generalized "pattern formation simulations" (PFS)

of the **Development** process. The PFS are based on the same set of geometric rules used on the CFS.

Figure 3b shows and example of PFS utilizing the full DNA ink mesh (Y_{ink} of 100 %) **Developed** with different OGNP sizes (5 nm and 10 nm OGNP in Figure 3, larger sizes shown in Figure S11). Our results indicate that smaller OGNP reproduce the DNA ink pattern more accurately. Small OGNP sizes prevent the zig-zag packaging effect and the multiple hybridizations per OGNP that we also observed in the chain pattern distorting the expected pattern appearance. In fact, our data suggest that to obtain geometrical features with resolutions comparable to the DNA ink mesh, the size of the OGNP (taking in account its minimal hydrodynamic radii) should be equal or smaller than the DNA ink spacing. For instance, a "hash 50 %" pattern **Developed** with 4 nm OGNP (Figure 3c), has full coverage of DNA ink pattern as compared to the more closely packed "hash 100 %" version (see Figure S11, 4 nm OGNP). The right panel of Figure 3c also illustrates how arbitrary shapes can be achieved by utilizing OGNP smaller than the DNA ink spacing.

The effect of Y_{ink} on a generalized mesh pattern was also investigated (see Figure S12). Again, achieving high Y_{ink} values is key to recover the pattern details after **Development**. These results corroborate the flexibility of the method to produce arbitrary geometries and highlight the importance of the efficiency of the DNA ink transfer and the geometrical restrictions imposed by the OGNP during the **Development** process in our set up. Future optimization of the DNA origami stamping method will use the *in silico* model to improve and apply these key aspects of nanoscale patterning on surfaces.

In conclusion, we have introduced a method that exploits DNA origami programmability to immobilize predefined DNA nanopatterns on surfaces. The possibility to create surfaces with spatial and sequence addressability with sub-10 nm range represents a step towards better resolution as compared with photoresist nanolithography,[22] processing robustness and control of surfaces.[12a] The **Stamping** of the DNA ink allows the

10

addressability of matter on surfaces within the nanoscale range without the necessity to have

the DNA nanostructure present; thus being compatible with conditions that usually would

affect the structural integrity of the DNA's secondary structure[23] or its interaction with the

surface.[24] Given that each staple in an origami structure has a unique sequence, it is

conceivable that hundreds of strands can be modified as DNA ink and subsequently

hybridized with any DNA linked molecules or nanomaterials of interest leading to a complex

addressable nanostructure. In addition to thiol groups, it is possible to immobilize the

oligonucleotides with other chemistries such as thiol-ene,[25] click chemistry,[26] amino

reactive groups[27] and on other surfaces such as silica, silicon nitride and polymeric surfaces.

This methodology could be implemented as an additional step in top-down methodologies[2c, 10] or the formation of periodic lattices.[14] Future studies could lead to the integration of this

methodology within multiplexed microfluidic[11] and more multipurpose read out systems,[10a]

For example, the integration of modular addressability with biological processes can be

utilized for the high throughput analysis of biochemical reactions and biomolecular

interactions that require control over proximity and special distribution. Thereby, the DNA

origami stamp method presented here brings the opportunity for a more versatile and robust

functionalization and patterning of surfaces for the creation of metamaterials[12a] with

applications in nanoelectronics[7] and photonics[2c]. Furthermore we show that the

immobilization process can be visualized by SPR opening the possibility for the development

of highly organized sensing surfaces.[5c,28]

Supporting Information

Supporting Information is available online from the Wiley Online Library or from the author.

[1]   a) N. C. Seeman, *Annu. Rev. Biochem* **2010**, *79*, 65; b) M. Tintoré, R. Eritja, C. Fàbrega, *ChemBioChem* **2014**, *15*, 1374.

[2]   a) J. Zheng, P. E. Constantinou, C. Micheel, A. P. Alivisatos, R. A. Kiehl, N. C. Seeman, *Nano Lett.* **2006**, *6*, 1502; b) R. Chhabra, J. Sharma, Y. Ke, Y. Liu, S. Rinker, S. Lindsay, H. Yan, *J. Am. Chem. Soc.* **2007**, *129*, 10304; c) A. M. Hung, C. M. Micheel, L. D. Bozano, L. W. Osterbur, G. M. Wallraff, J. N. Cha, *Nat Nanotechnol* **2010**, *5*, 121; d) S. Pal, Z. Deng, B. Ding, H. Yan, Y. Liu, *Angew. Chem. Int. Ed. Engl.* **2010**, *49*, 2700; e) P. K. Dutta, R. Varghese, J. Nangreave, S. Lin, H. Yan, Y. Liu, *J. Am. Chem. Soc.* **2011**, *133*, 11985; f) A. Kuzyk, R. Schreiber, Z. Fan, G. Pardatscher, E.-M. Roller, A. Högele, F. C. Simmel, A. O. Govorov, T. Liedl, *Nature* **2012**, *483*, 311.

[3]   P. W. K. Rothemund, *Nature* **2006**, *440*, 297.

[4]   S. M. Douglas, H. Dietz, T. Liedl, B. Högberg, F. Graf, W. M. Shih, *Nature* **2009**, *459*, 414.

[5]   a) J. Fu, M. Liu, Y. Liu, N. W. Woodbury, H. Yan, *J. Am. Chem. Soc.* **2012**, *134*, 5516; b) B. Sacca, R. Meyer, M. Erkelenz, K. Kiko, A. Arndt, H. Schroeder, K. S. Rabe, C. M. Niemeyer, *Angew. Chem. Int. Ed. Engl.* **2010**, *49*, 9378; c) M. Tintoré, I. Gállego, B. Manning, R. Eritja, C. Fàbrega, *Angew. Chem. Int. Ed.* **2013**, *52*, 7747.

[6]   R. Schreiber, J. Do, E. M. Roller, T. Zhang, V. J. Schuller, P. C. Nickels, J. Feldmann, T. Liedl, *Nat Nanotechnol* **2014**, *9*, 74.

[7]   H. T. Maune, S. P. Han, R. D. Barish, M. Bockrath, W. A. Iii, P. W. Rothemund, E. Winfree, *Nat Nanotechnol* **2010**, *5*, 61.

[8]   R. J. Kershner, L. D. Bozano, C. M. Micheel, A. M. Hung, A. R. Fornof, J. N. Cha, C. T. Rettner, M. Bersani, J. Frommer, P. W. Rothemund, G. M. Wallraff, *Nat Nanotechnol* **2009**, *4*, 557.

[9]   N. V. Voigt, T. Torring, A. Rotaru, M. F. Jacobsen, J. B. Ravnsbaek, R. Subramani, W. Mamdouh, J. Kjems, A. Mokhir, F. Besenbacher, K. V. Gothelf, *Nat Nanotechnol* **2010**, *5*, 200.

[10]   a) M. B. Scheible, G. Pardatscher, A. Kuzyk, F. C. Simmel, *Nano Lett.* **2014**, *14*, 1627; b) A. Gopinath, P. W. Rothemund, *ACS Nano* **2014**, *8*, 12030.

[11]   K. Hsieh, B. S. Ferguson, M. Eisenstein, K. W. Plaxco, H. T. Soh, *Acc. Chem. Res.* **2015**, *48*, 911.

[12]   a) A. V. Kildishev, A. Boltasseva, V. M. Shalaev, *Science* **2013**, *339*, 1232009; b) N. Yu, F. Capasso, *Nat Mater* **2014**, *13*, 139.

[13]   S. Perez-Rentero, S. Grijalvo, G. Peñuelas, C. Fàbrega, R. Eritja, *Molecules* **2014**, *19*, 10495.

[14]   S. Woo, P. W. Rothemund, *Nat Commun* **2014**, *5*, 4889.

[15]   A. V. Pinheiro, D. Han, W. M. Shih, H. Yan, *Nat Nanotechnol* **2011**, *6*, 763.

[16]   E. Stenberg, B. Persson, H. Roos, C. Urbaniczky, *J. Colloid Interface Sci.* **1991**, *143*, 513.

[17]   A. V. Garibotti, X. Sisquella, E. Martínez, R. Eritja, *Helv. Chim. Acta* **2009**, *92*, 1466.

[18]   C. A. Mirkin, R. L. Letsinger, R. C. Mucic, J. J. Storhoff, *Nature* **1996**, *382*, 607.

[19]   D. A. Giljohann, D. S. Seferos, A. E. Prigodich, P. C. Patel, C. A. Mirkin, *J. Am. Chem. Soc.* **2009**, *131*, 2072.

[20]   H. Chen, X. Kou, Z. Yang, W. Ni, J. Wang, *Langmuir* **2008**, *24*, 5233.

[21]   S. Takabayashi, W.P. Klein, C. Onodera, B. Rapp, J. Flores-Estrada, E. Lindau, L. Snowball, J. T. Sam, J.E. Padilla, J. Lee, W.B. Knowlton, E. Graugnard, B. Yurke, W. Kuang, W.L. Hughes *Nanoscale*, **2014**, *6*, 13928.

[22]   a) D. Pasini, J. M. Klopp, J. M. J. Fréchet, *Chem. Mater.* **2001**, *13*, 4136; b) J. M. Klopp, D. Panisi, J. D. Byers, C. G. Wilson, J. M. J. Fréchet, *Chem. Mater.* **2001**, *13*, 4147.

[23]   I. Mamajanov, A. E. Engelhart, H. D. Bean, N. V. Hud, *Angew. Chem. Int. Ed.* **2010**, *49*, 6310.

[24]   I. Gállego, M. A. Grover, N. V. Hud, *Angew. Chem. Int. Ed.* **2015**, *54*, 6765.

[25]   J. Escorihuela, M.J. Bañuls, S. Grijalvo, R. Eritja, R. Puchades, A. Maquieira, *Bioconjug. Chem.* **2014**, *25*, 618.

[26]   S. Oberhansl, M. Hirtz, A. Lagunas, R. Eritja, E. Martínez, H. Fuchs, J. Samitier, *Small*, **2012**, *8*, 541, P. Jonkheijm, D. Weinrich, H. Schröder, C.M. Niemeyer, H. Waldmann, Angew. Chem. Int. Ed. 2008, 47, 9618.

[27]   B. Manning, S.J. Leigh, R. Ramos, J. Preece, R. Eritja, R. *J. Exp. Nanoscience*, **2010**, *5*, 26; M. Manning, G. Redmond, *Langmuir* **2005**, *21*, 395.

[28]   a) Y. Ke, S. Lindsay, Y. Chang, Y. Liu, H. Yan, *Science* **2008**, *319*, 180; b) H. K. Subramanian, B. Chakraborty, R. Sha, N. C. Seeman, *Nano Lett.* **2011**, *11*, 910.
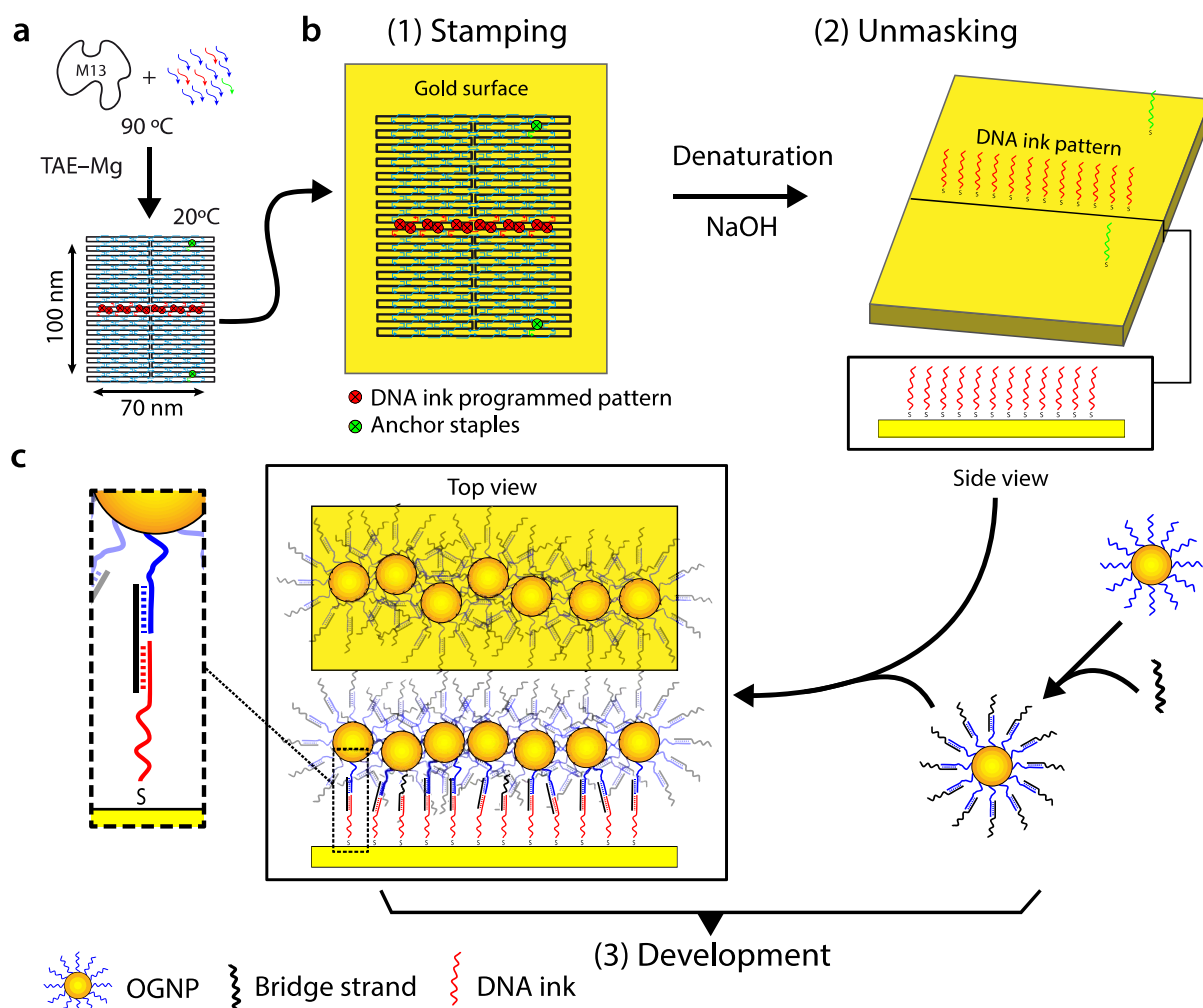
Scheme 1. Stamping methodology to transfer DNA origami pattern information to surfaces a) DNA origami stamp design and assembly process. b) DNA origami Stamping process of a linear DNA ink programmed pattern on gold surfaces (see Supporting Information for detailed protocol). The protocol describes the three basic steps of the: Stamping (1), Unmasking (2) and Development (3). (1) DNA origami stamp is adsorbed on gold surfaces in the presence of 125 mM magnesium for least 30 min. Then the DNA stamp is left over the surface until the thiol groups of the ink and anchor staples react with the gold surface. (2) The frame of the DNA stamp is denatured with NaOH and rinsed out to expose the DNA ink pattern. The DNA bridge was annealed directly to the OGNP. Finally, the pattern is developed with the annealing of the OGNP-bridge sequence to the surface (3). c) Detail of the Gold surface–DNA ink–Bridge sequence–OGNP sandwich in step (3).
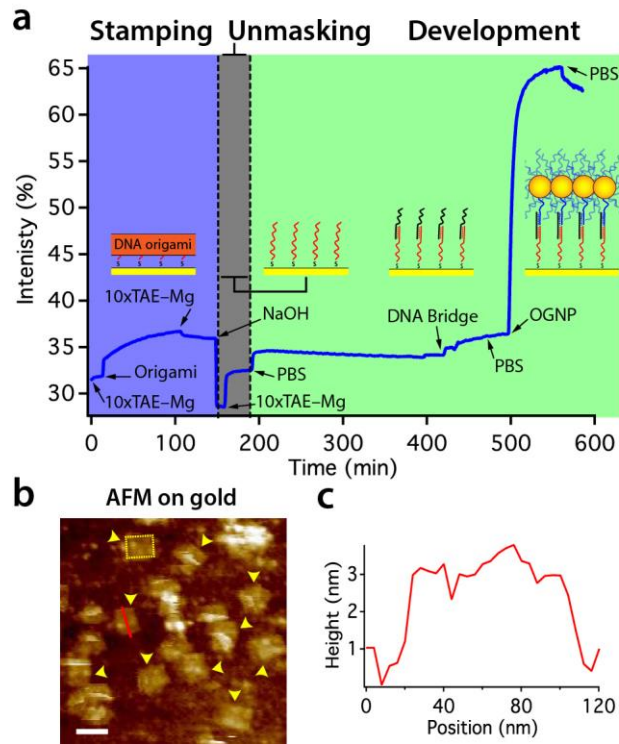
Figure 1. Characterization of the DNA ink stamp process. a) SPR analysis of Stamping, Unmasking and Development. The intensity of refracted light was monitored at a constant angle (see Supporting Information for details) during the process of addition of buffers and the different components necessary for the process, as indicated with arrows through the SPR profile upon time. The increase in the refracted intensity indicates adsorption of matter over the gold surface and the decrease indicates desorption. 10xTAE–Mg indicates the point of addition of buffer containing 125 mM Mg^{2+} and PBS indicates the addition of phosphate buffer 10 mM (see Supporting Information for details). b) AFM image in liquid of the DNA origami stamp on annealed gold after 30 min of adsorption in the presence of 125 mM Mg^{2+}. The yellow rectangle depicts a DNA origami frame domain (100 nm x 70 nm) for comparison with the DNA origami stamps imaged on gold the surface. The yellow arrowheads point some the DNA origami stamps over the gold surface. Scale bar: 100 nm. c) Height profile of a DNA origami stamp section delimited by the red line in (b).
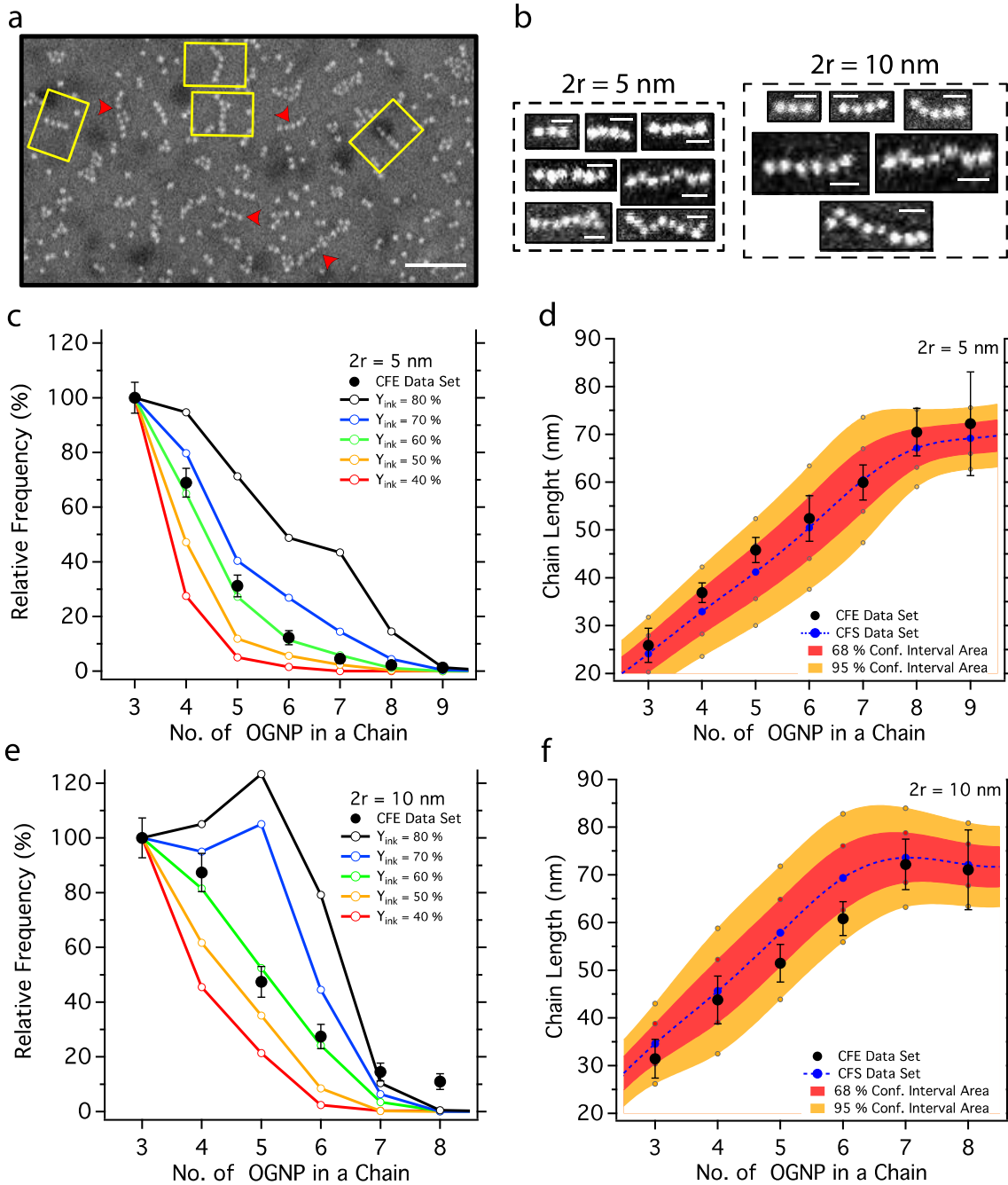
Figure 2. CFE (experiments) and CFS (simulations) OGNP chain-formation analysis. a) SEM image of 10 nm OGNP aligned with the DNA origami stamp method. The yellow rectangles depict the DNA origami stamp frame domain (100 nm x 70 nm). Red arrowheads point some OGNP chain alignment. Scale bar: 100 nm. b) SEM images corresponding to different chain classes (i.e. different numbers of OGNP aligned in a chain) obtained after performing a CFE using 5 nm and 10 nm particles. 2r indicates the diameter of the gold nanoparticles, as it relates to its mathematical definition in the *in silico* model (Supporting Information). Scale bars: 20 nm. c) shows the analysis of the relative frequency of number of OGNPs in a chain and (d) the length distribution of the chains for the CFE and CFS results utilizing 5 nm OGNP in the Development step. (e) and (f) show the same analysis but utilizing 10 nm OGNP in the Development step. Relative frequencies for CFE data in (c) and (e) were calculated from a total of n = 844 independent chain formation events, for both OGNP diameter (see Supporting Information). CFS data set for the length analysis in both OGNP diameters corresponds to

CFS runs with Y_{ink} = 60 %. Circle hollow markers on CFS data set and in confidence intervals indicate the data points used for obtaining the interpolation curves depicted in the (d) and (f) panels. Confidence interval values are calculated for each class of OGNP chain.
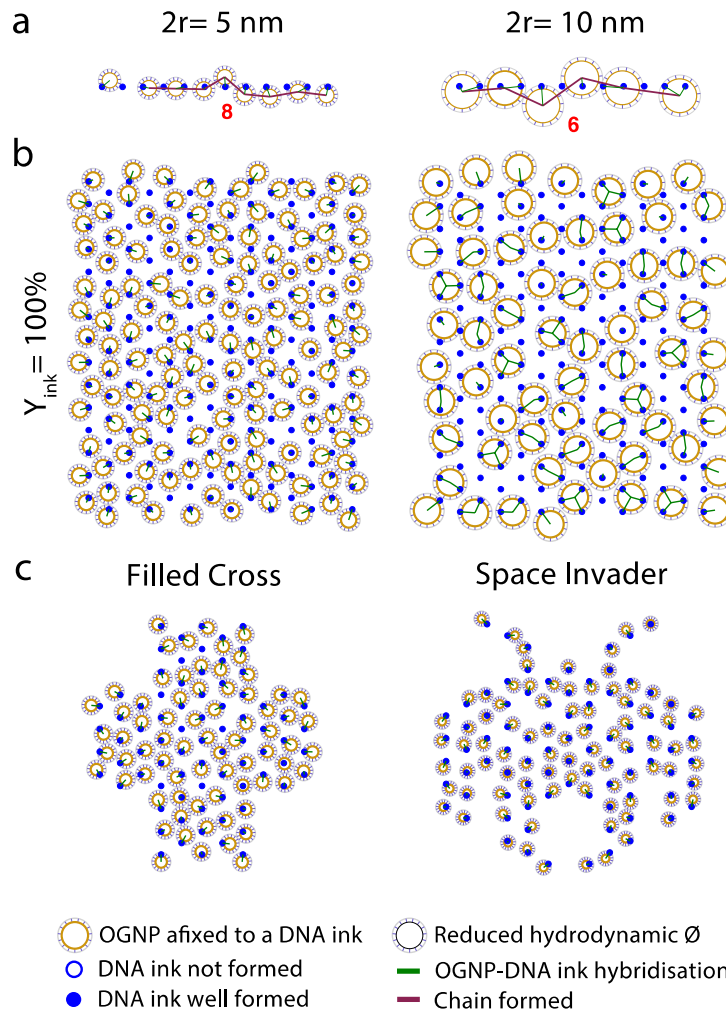

Figure 3. *In silico* Development of the chain and the mesh-like DNA ink patterns. a) Selected results of CFS using 5 and 10 nm OGNP. The centers of the OGNP have been linked with a violet line to highlight the chain paths formed. The figures in red indicate the number of OGNP contained in the chain. b) Montecarlo PFS Simulations showing the effect of the OGNP diameter on the Development process of a full mesh of DNA ink within the DNA origami design. The simulation assumes 100 %-yield of DNA ink well formed. c) Montecarlo PFS Simulations of the Development of the indicated DNA ink patterns (Y_{ink} = 100 %) using 4 nm (hash 50%) and 3 nm (space invader) OGNPs.
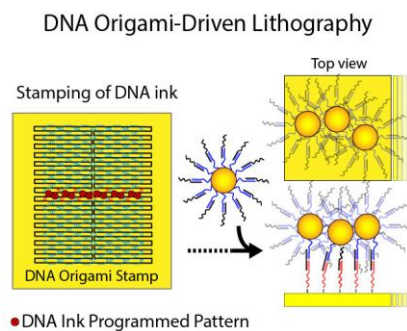
The table of contents entry Sub-10 nm lithography of DNA patterns is achieved using the DNA origami Stamping method. This new strategy utilizes DNA origami to bind a preprogrammed DNA ink pattern composed of thiol-modified oligonucleotides on gold surfaces. Upon denaturation of the DNA origami the DNA ink pattern is exposed. The pattern can then be developed by hybridization with complementary strands carrying gold nanoparticles.

Isaac Gállego,* Brendan Manning, Joan Daniel Prades, Mònica Mir, Josep Samitier and Ramon Eritja*

Title (**DNA Origami-Driven Lithography for Patterning on Gold Surfaces with Sub-10 Nanometer Resolution**)

ToC figure ((55 mm broad, 50 mm high, or 110 mm broad, 20 mm high))

Supporting Information

DNA Origami-Driven Lithography for Patterning on Gold Surfaces with Sub-10 Nanometer Resolution

By Isaac Gállego,* Brendan Manning, Joan Daniel Prades, Mònica Mir, Josep Samitier and *Ramon Eritja**

Table of contents:

Figure List:

Table List:

1. General Methods

Thiolated oligonucleotides shown in Table S1 are from IDT technologies. Unmodified oligonucleotides (Tables S2-S3) (Sigma) and M13mp18 (New England Biolabs) were used as received. The rest of the chemicals are analytical reagent grade.

All the glassware used in this work was cleaned with piranha solution (70% H_2SO_4, 30% H_2O_2; v/v) for 15 minutes. Then it was rinsed with two volumes of nanopure water, and then, sonicated for 15 minutes in a volume of nanopure water. Then, it was rinsed with two volumes of ethanol (analytical grade) and sonicated for 30 minutes in ethanol. After the sonication, the glassware was dried at 127ºC for at least 24 h prior to use.

Use of 10 x TAE-Mg: The use of this amount of buffer when high $MgCl_2$ is required is an artefact of experimental convenience: the stock solution (10 x TAE, 125 mM $MgCl_2$) used in the preparation of 1x TAE, 12.5 mM $MgCl_2$ formation buffer for the DNA origami was readily at hand for it use.

2. Preparation of DNA origami

Tall rectangle DNA origami tiles were assembled following the method developed by Rothemund.[3] A mixture containing the viral DNA and all the staple strands at a molar ratio of 1:10 was heated on a Biorad Termocycler at 90ºC and slowly cooled to 20ºC at -1ºC/minute (buffer conditions: 40 mM Tris with 20 mM EDTA and 12.5 mM $MgCl_2$). In the case of the thiol-modified origami, the appropriate unmodified staple strands were replaced by the 14 thiol-modified ink staples (Table S1). The ink staples were modified in the 5' end introducing an oligothymidine spacer (9 or 10 bases) followed by a disulfide modification. According to the design, the 5'-end of all the staples that compose the DNA origami are facing the same plane of the structure. The disulfide modification was incorporated using the 5'-thiol modifier-C6 S-S CE phosphoramidite. The left most and the right most column of staples of the design where excluded to avoid lateral stacking of the DNA origami. The assembled DNA origami were purified from excess staple strands using Microcon centrifugal filter devices (100K MWCO; Millipore) as follows: centrifugation at $\leq$ 5000 g during 10-15 min and repeat process 2x adding 1x TAE-Mg at each step. The resulting solution containing purified origami was used for the next steps.
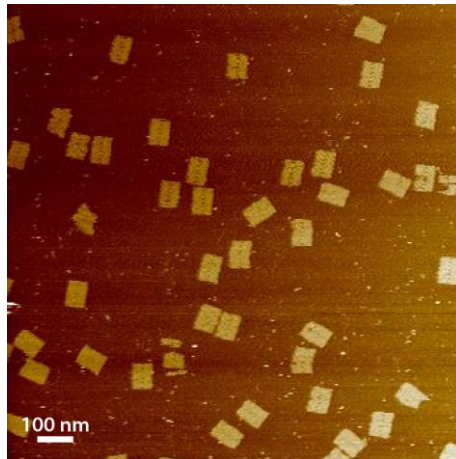
Figure S1: AFM image in liquid of the DNA origami stamp over mica surface. The DNA origami sample imaged has been previously purified with the MWCO filter to eliminate the excess of DNA ink staples.
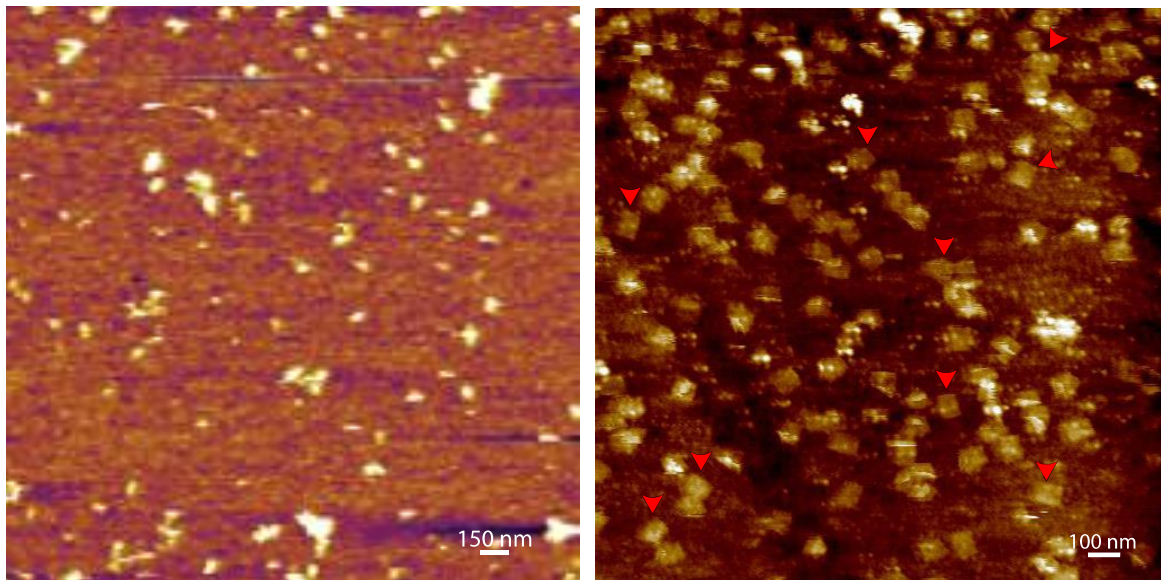
Figure S2: Comparative AFM imaging of non-modified and thiol-modified DNA origami stamp on gold surfaces. No well resolved DNA origami structures could be observed when non-modified DNA origami stamp were adsorbed on gold surfaces (left panel). When thiol-modified staples were introduced in DNA origami stamp, was possible to visualize of the nanostructures (red arrow heads point some of the nanostrucures) on gold surfaces (right panel).

3. Functionalization of Gold Nanoparticles (GNP)

Citrate stabilized gold nanoparticles (5 or 10 nm) were purchased from BBI Life Sciences and used as received. To prepare the conjugates, 1.5 molar excess of thiol- oligonucleotide (DNA-CG: 5'-<u>TGACTCAATGACTCG</u>TTTTTTTTTTT-3'-phosphate-$(CH_2)_3$-SH), to respect maximum theoretical load of oligonucleotide according to described protocols,[29]

dissolved in water was added to the colloidal gold solution. The mixture was slowly shaken by rotation for 16 h at room temperature (RT). Then the solution was brought to a final concentration of 10 mM sodium phosphate (pH = 7.2) and 0.1 M NaCl in a stepwise fashion. The mixture was then mixed slowly by rotation for 24 h. Finally, to remove the excess of oligonucleotide, the solution was centrifuged at 20000 *g* and 20 ℃ for 30 min. The supernatant was removed and the red oil in the bottom of the centrifuge tube, containing the oligonucleotide–GNP, was resuspended in the appropriate volume with 0.1 M NaCl, 10 mM sodium phosphate buffer (pH = 7.2). The centrifugation and suspension process was repeated twice, finally dissolving the OGNP in 0.5×TBE (45 mM Tris-borate, 1 mM EDTA), 50 mM NaCl. The resulting OGNP were passivated with O-(2-Mercaptoethyl)-O′-methyl-hexa(ethylene glycol) (OEG-thiol).[19] Then, 1/10 of 20 µM OEG-thiol solution in water was added to the OGNP. After incubation with vigorous shaking at RT for 3 hours, the suspension was centrifuged in the same conditions described above. The final resuspension was held in 1xTBE, 0.1 M NaCl (pH = 7.2), containing 0.1% NaN$_3$ and then was stored in the fridge (4 °C) prior to use.

The different steps of the OGNP synthesis were followed by agarose gel 3% in 0.5X TBE at 10 V/cm for 45 min. To allow gel electrophoreses of the parent particles the GNP's were stabilized by exchange of the commercial citrate by 4,4′-(phenylphosphinidene)bis(benzenesulfonic acid) (Phosphine) using standard protocols.[30]
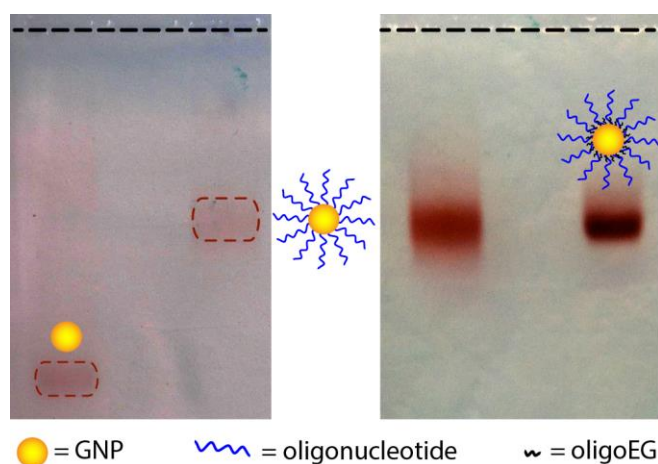

Figure S3 Agarose gel images of the synthesis of the 5 nm OGNP. The two central bands correspond to the gold nanoparticle (GNP) coated with the oligonucleotides as reference for comparison. The dashed line on the top indicates the position of the loading pockets. EG stands for polyethylene glycol.

4. Surface Plasmon Resonance (SPR) characterization

All the steps required for the DNA origami stamp process on the gold surface were monitored and quantified by SPR. The SPR substrates were ~50 nm evaporated gold films on BK7 glass with ~2 nm of chromium in order to improve adhesion between the gold and glass. SPR was performed in the Kretschmann configuration with a setup from Resonant Technologies GmbH. The instrument contains a HeNe laser operating at $\lambda = 632.8$ nm that passes a chopper, the polarizer intensity and control polarizer before being reflected on the base of a 90° high index glass prism. The photodiode collects the reflected light and the intensity is monitored as a function of the angle of incidence, obtaining the angular reflectivity scans. The intensity is also monitored as function of time at a fixed angle of incidence (30 % below the maximum of resonance) in the kinetic measurements.

All the incubation steps were monitored continuously and angular reflectivity scans were performed before and after each incubation step. The buffer used in the DNA origami mixture, 400 mM Tris with 20 mM EDTA and 125 mM $MgCl_2$ (10x TAE-Mg), was used as a baseline in the SPR chip, when a stable signal was observed the origami DNA mixture was added into the SPR cell for 1.5 hours. The DNA origami covalently attached on the gold surface was denatured after 10 minutes in the presence of 50 mM NaOH. The attached oligonucleotides were hybridised for 1 hour with a complementary strand (1 µM) in 10 mM phosphate buffer, 3 mM KCl and 137 mM NaCl at pH 7.4 (PBS) and then hybridized for the same time with the 10 nm OGNP (1 µM) in PBS.

All the steps were performed under a flow rate of 60 µL/ min and between each step the chip was rinsed with 5 mM NaH_2PO_4, 1 mM KCl, 700 mM NaCl, 0.03% Tween 20 at pH: 7.42 (washing buffer), to remove non–specifically bound molecules.
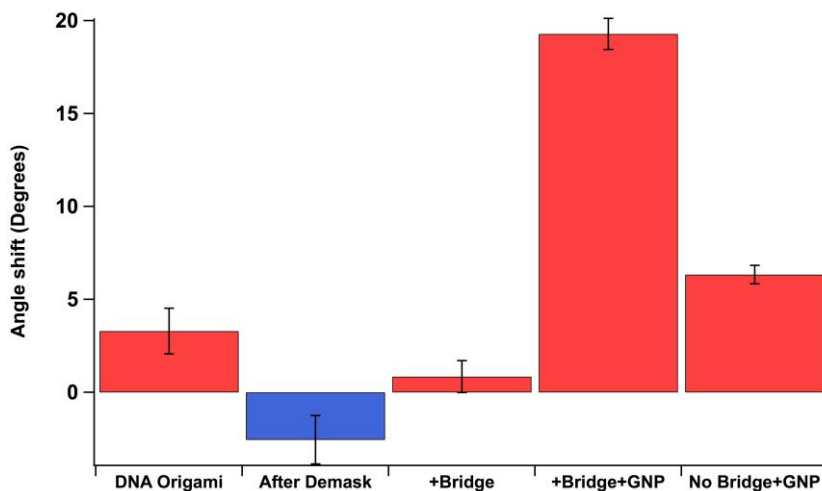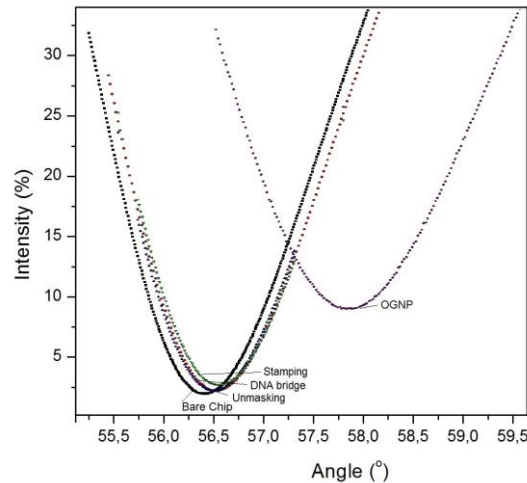
Figure S4: Refractive angle shift analysis for each step of the DNA origami stamp process using SPR

5. Atomic Force Microscopy (AFM) imaging

AFM imaging was performed on the DNA origami sample preparation described in section 2. The AFM on mica was performed after each preparation for control of the annealing. 1 µL of sample containing purified DNA origami was spotted on freshly cleaved mica (Ted Pella, Inc.) and left to adsorb for 1 min. Then 40-50 µL of 1X TAE-Mg was added to perform the imaging. The preparation of sample on gold surfaces was performed as follows: 3-4 µL of sample containing purified DNA origami stamp was deposited on clean annealed gold (Arrandee) and left to adsorb for 3 min. Then 40-50 µL of 10x TAE-Mg was added, and the solution was left to adsorb for 30 min before imaging. AFM images in tapping on air were performed on each annealed gold surface as control before use. All AFM images were obtained on a Multimode microscope attached to a Nanoscope III electronics (Veeco). Images were acquired in tapping mode in liquid using triangular-shaped SNL-10 probes (Bruker) with a nominal spring constant of 0.35 N/m, or in tapping mode in air with rectangular-shaped T-190 probes (Vistaprobes) with a nominal spring constant of 48 N/m.

6. Scanning Electron Microscopy (SEM) characterization

Prior to use, gold surfaces over glass (Arrandee) were cleaned with washes in MQ water / ethanol and then annealed as described elsewhere. Briefly: Arrandee gold was heated until glowing red, then allowed to cool for about 30 seconds. Heating and cooling process was repeated about 3-4 times. Immediately after final heating, gold surface was quenched by addition of 20-30 μL of MQ water and left to cool down, and finally rinsed with MQ water. All annealed gold used in this work was imaged by AFM on air to ensure flat terraces formation after annealing and cleanness of the surface.

A 3-4 μL–drop of purified DNA origami stamp was spotted on a clean freshly annealed gold surface (Arrandee) and left to adsorb for 3 minutes. Afterwards, 40-50 μL of 10xTAE–Mg containing 125 mM Mg^{2+} was added and the sample was then incubated for 5–6 hours in a humid environment in a Petri dish. The gold surface was briefly soaked in a solution of 50% EtOH/water (v/v), immersed in a clean vial with approx. 2 mL of 10xTAE–Mg and then incubated at RT for 5 days protected from light. The additional EtOH/water step was added to fix the DNA origami on the gold surface increasing the number of DNA origami covalently attached. After the long incubation, the sample was then immersed in a glass vial containing 0.1 M NaOH for 30 minutes while the sample was agitated slowly. The sample was then carefully rinsed with 2 mL of nanopure water and finally placed in a glass vial covered with nanopure water for 30 minutes. Afterwards, the gold surface was removed and rinsed with 1xPBS, 0.025% SDS, and the excess of buffer was removed carefully contacting the side of the surface with a filter paper (Whatman) without drying off totally the sample. Then 20 μL of a 10 nM solution of OGNP (10 nm or 5 nm of diameter) containing the twelve bridge sequences complementary to the DNA ink in 1x PBS, 0.025% SDS was added on the surface and left to hybridize in a humid environment in a Petri dish for 3 hours at RT.

The twelve Bridge sequences were previously hybridized with the OGNPs as follows: a solution of 0.5 μM of each of the twelve bridge sequences where mixed with 10 nM OGNP in 1x PBS, 0.025% SDS. The mixture was sonicated for 5 seconds and then was heated for 5 minutes at 60ºC and cooled down and sit for at least 30 minutes at RT. Then, the mixture was centrifuged at 16000 g at 20 ºC for 20–30 minutes. The supernatant was discarded and the pellet was resuspended in 1x PBS, 0.025% SDS with 2–3 times the initial volume. The centrifugation/centrifugation step was repeated three times and the OGNP-Bridge suspension

was finally suspended in the initial amount of volume. After annealing process of the OGNP–Bridge, the gold surface was rinsed off carefully of the OGNP bridge excess with 1xPBS, 0.025% SDS and finally was washed with 0.3 M ammonium acetate and left to dry at RT until imaging. The SEM imaging was performed using a Nova NanoSEM 230 (FEI) operated at 5-10 kV.
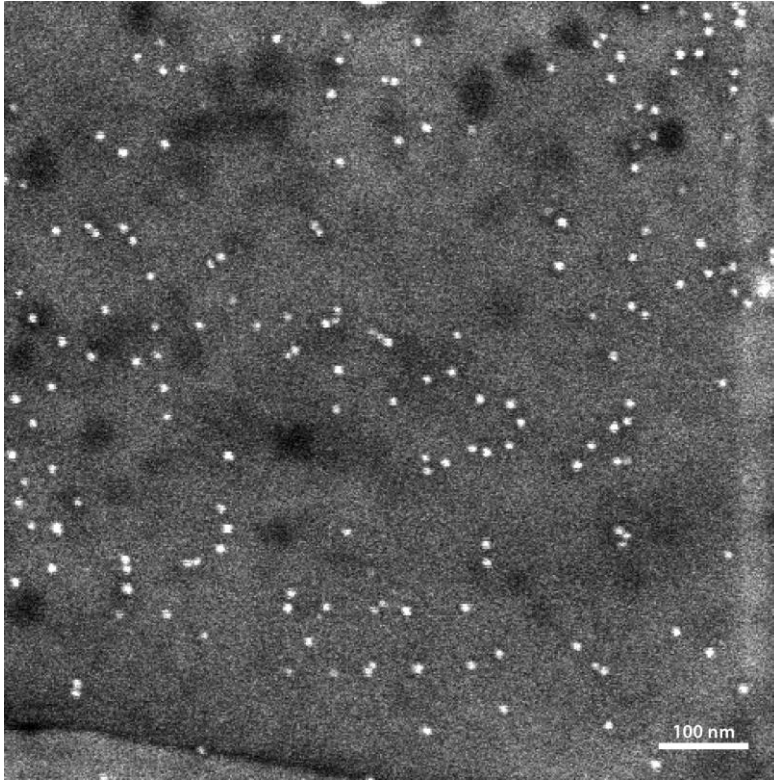

Figure S5: Control image of a gold surface that was subjected to all the Stamping steps but without the addition of the DNA origami stamp.
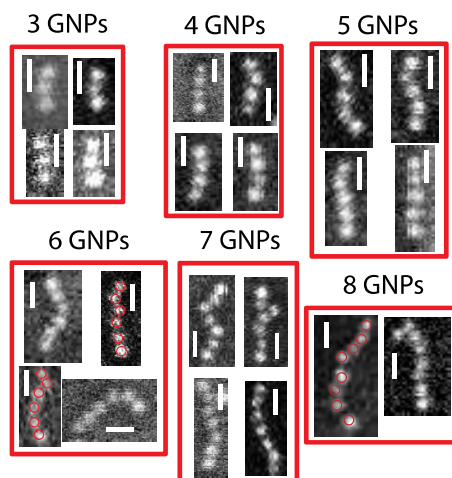
Figure S6: Selection of SEM images of the alignment of 5 nm GNPs over annealed gold using the DNA origami stamp method. Scale bars: 20 nm.
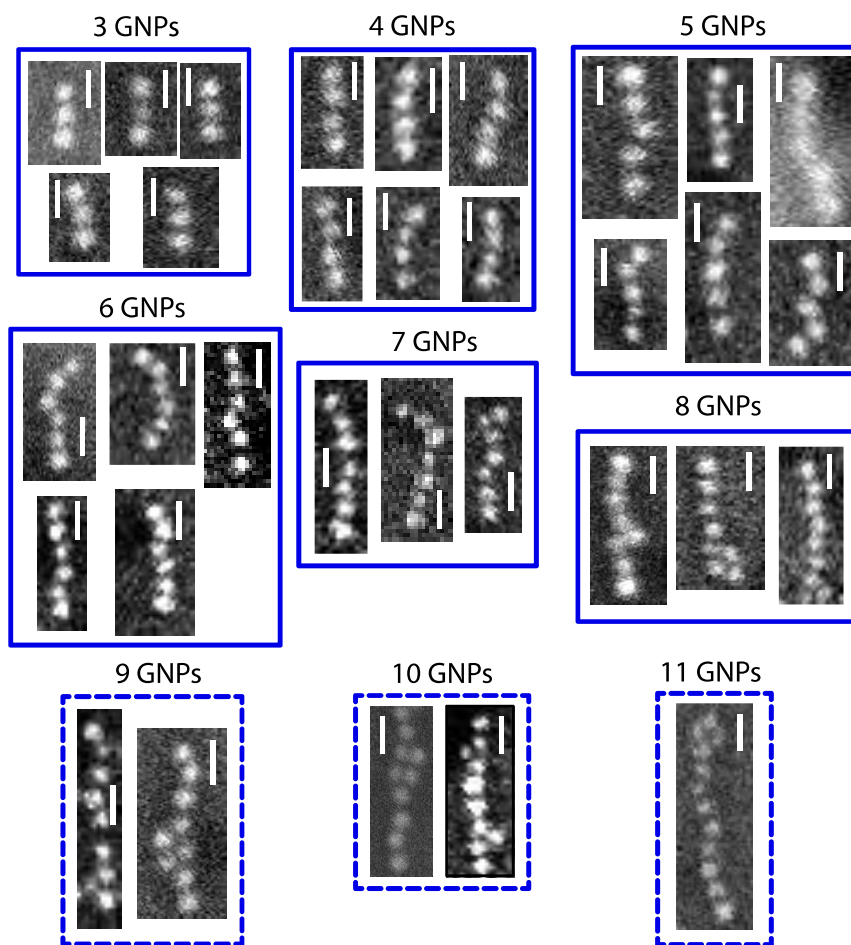
Figure S7: Selection of SEM images of the alignment of 10 nm OGNPs on annealed gold using the DNA origami stamp method. Scale bars: 20 nm. Chain images with > 9 OGNP per chain (within discontinuous frame), are examples of chains that were present in very low frequency and that were not detectable in CFS runs (see section 8 of SI for more details).

7. Statistics

Statistical analysis was performed on SEM images from different fields of each sample analyzed using visual inspection to determine the number of OGNP participating in each alignment. SEM images were first subjected to minimal editing in Photoshop to maximize the contrast between the particles and background. The number of aligned OGNP for each class (# of particles in a chain) were counted using the cell counter plugin for FIJI (NIH).[31] A total of n = 844 chain formation events were studied for each diameter of OGNP to obtain the relative frequencies of the CFE in Figure 2. The number of events for the 3 OGNP chain class was of n = 384 (2r = 5 nm) and of n = 287 (for 2r = 10 nm).

8. Montecarlo simulations

8.a. Model fundamentals

Montecarlo Simulations (MS) designate statistical methods for solving problems ruled by a set of logic or mathematical laws. MS is especially suited for predicting macroscopic trends emerging from a number of superimposed microscopic processes. In our case, we aimed at predicting the relative frequency distribution of different chain lengths —defined by the number of nanoparticles aligned– observed in SEM images.

Our model builds upon the assumption that the chain formation process can be considered additive, affixing one OGNP after another at the DNA ink sites. The arrival and hybridization of a new OGNP is thus influenced by the presence of other OGNPs attached before. To explain this, we assumed a simple set of rules:

A. An OGNP can *approach the surface* **only if** there is *enough room* around its landing position (i.e. there is enough room left by previous nanoparticles to accommodate it).

B. Once approached to the surface, an OGNP *attaches to* it **only if** a *vacant DNA ink site is at reach*.

Following these two rules, chain formation simulations (CFS) mimicked *in silico* the chain formation experiments (CFE), throwing a large number of OGNPs (*N*), one after the other, to random landing positions around one single DNA origami structure. Individual CFS-runs were repeated (*M*) to account for the diversity of OGNP chain arrangements that could be formed by this random procedure. Statistic results were finally extracted from the ensemble of CFS. Figure S8 shows the geometry considered for the problem and many examples of individual CFS runs for clarity.

8.b. Model details

DNA ink sites were aligned at evenly spaced positions, following the geometry defined by DNA origami (a total of 12 DNA ink sites with a 5.44 nm spacing).

OGNP landing positions *(x_i,y_i)* were randomly generated in 2 dimensions, with a uniform distribution, in the vicinity of the DNA origami. For computational economy, only positions that could lead to an interaction between OGNPs and ink sites were considered. (i.e. no farther than half the OGNP size (*$\Sigma/2$*) from the DNA ink sites, see Eq.(IV) below).

OGNP size Σ accounted for their nominal radius (*r*, this was 2.5 nm and 5 nm in our experiments) plus a spherical shell *s* of approximately 2 nm. The spherical shell corresponds to a pseudo hydrodynamic space fulfilled by the oligonucleotides linked to the OGNP. We chose such short additional length because oligonucleotides attached to a gold nanoparticle can be pushed and squeezed upon mechanical restrictions reducing dramatically the hydrodynamic diameter of the oligonucleotide-GNP particles.[21,32] Overall, sizes $\Sigma = 2\cdot(r + s)$ of 9 nm and 14 nm were used.
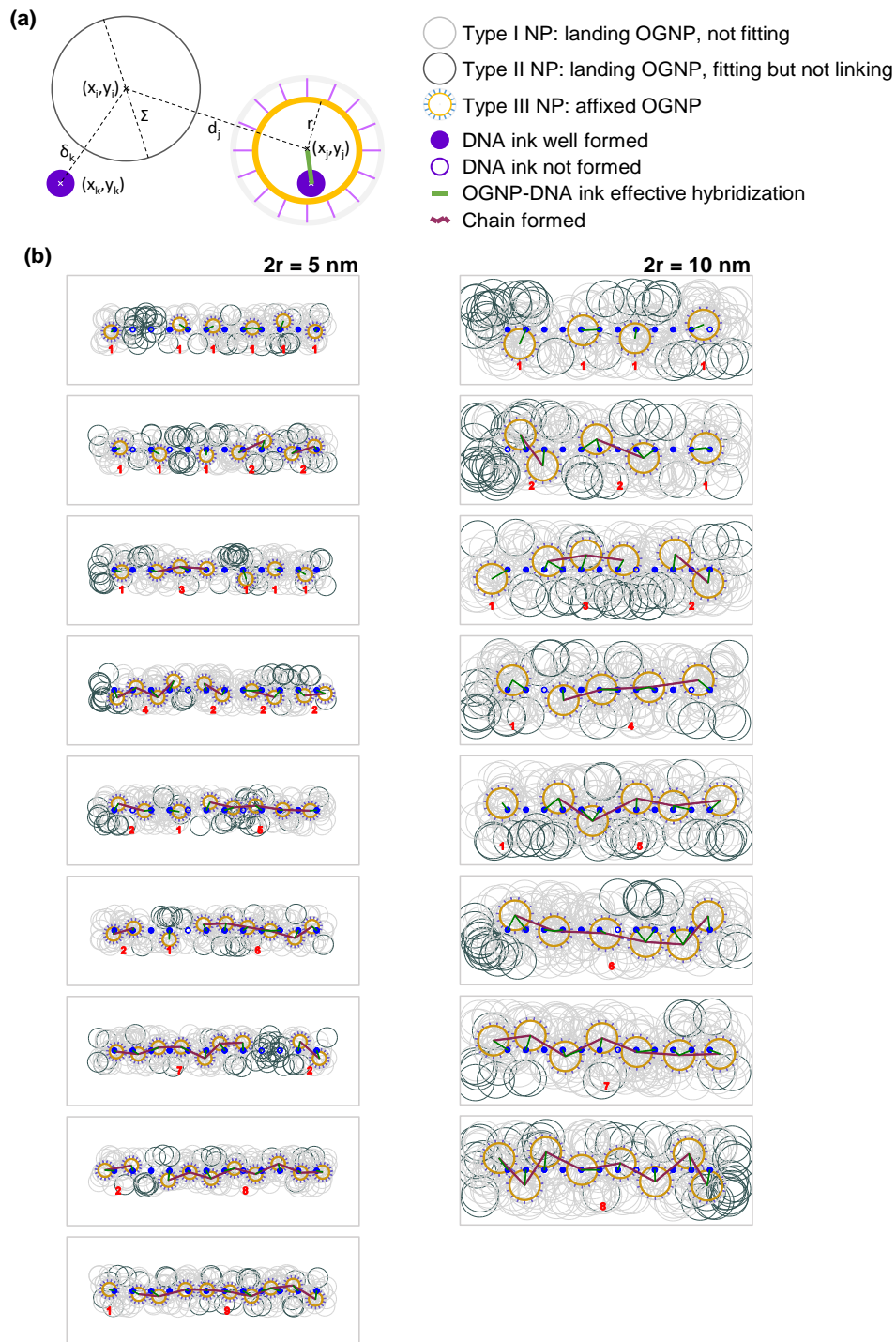
Figure S8: Model and example of chains formed in the CFS. (a) Sketch of the geometry used in the model: two DNA ink sites, one linked to an OGNP (yellow circle); then, a new OGNP that binds (dark grey circle). Main positions and distances are indicated. Color/symbol code used in (a) and (b) is given on the right side of (a). (b) Examples of CFS runs for 5 nm (left panels) and 10 nm (right panels) OGNP. In each CFS, N = 200 OGNPs were thrown to random positions onto twelve ink sites formed at different Y_{ink} rates. Type I OGNPs represent particles that have landed close to DNA ink but do not fit because are blocked by previously arrived particles. Type II GNPs fitted in free regions but had no

access to well-formed, free DNA inks. Type III OGNP are successfully affixed to the surface (hybridized either to 1 or 2 DNA inks) and are forming a chain. Type III OGNPs show the gold nanoparticle (gold circle) and the shell created by oligonucleotides attachment (external grey circle filled with radially distributes lines). For clarity, the number of OGNPs forming each detected chain is indicated in red.

First, rule A was applied for each new OGNP. For the i-th OGNP, after generating its landing position (x_i, y_i), we calculated the Euclidean distances d_j to the rest of OGNPs as:

$$d_j = \sqrt{(x_i - x_j)^2 + (y_i - y_j)^2} \quad \forall j \neq i \tag{I}$$

with j running for all other OGNPs. The OGNP **fitted only if** all d_j distances were larger than the OGNP size Σ. This is:

$$d_j \geq \Sigma \quad \forall j \neq i \tag{II}$$

In that case, the OGNP was allowed to land (Type II), continuing to verify rule B. If the OGNP did not fit, it was just discarded (Type I), proceeding with a new one.

Second, to verify rule B, we calculated the Euclidean distances δ_k to all the available DNA ink sites as:

$$\delta_k = \sqrt{(x_i - x_k)^2 + (y_i - y_k)^2} \quad \forall k \tag{III}$$

with k running for the DNA ink sites located at (x_k, y_k) respectively. The OGNP was then attached to the surface, **only if at least one** available DNA in site was at reach (i.e. one link would be formed). *Available* meant that the DNA ink was *well formed* (see below for more details) and *not previously hybridized* to another OGNP. *At reach* meant that it was *laying under the OGNP*. This is

$$\delta_k \leq \frac{\Sigma}{2} \tag{IV}$$

If this second condition was satisfied, the OGNP was affixed to the surface at its initial landing position, blocking the space around for further OGNPs, and consuming the DNA inks involved in the formed links (Type III OGNP).

Our model is self-limiting. After multiple OGNP have landed (N OGNP thrown), no more OGNPs can find either room (rule A) or accessible links (rule B). Therefore, the final chain configuration will mainly depend on the particular set of landing positions generated through the sequence. This way, the CFS model mimics the CFE self-assembly process on one single DNA origami structure. From a computational point of view, one could run this model a

number of times (*M* model runs) to generate statistics about the different chains that could possibly be generated.

Full-length chain formation was evaluated experimentally from CFE using SEM images of OGNP chains. The maximum apparent number of OGNP in a chain that a DNA origami domain can contain was obtained by counting the number of aligned OGNP when superimposing a DNA origami frame on them. This method lead to chains made of up to 9 and 8 OGNP in the 5 nm and 10 nm experiments, respectively. Longer chains were very rare, and always contained extremely closed packed configurations (e.g. double OGNP row chains) (see discontinuous framed configurations in Figure S7). These arrangements had almost negligible frequency in the CFE experiments (<0.1%) and never appeared in the CFS runs (0.0%). This is because, double row arrangements, with OGNP circles tangent to the line of DNA ink sites, are not compatible with the geometric constrains imposed on our *in silico* model.

DNA ink yield (Y_{ink}) was defined as the apparent fraction of well-formed DNA ink sites; this is, capable of hybridizing with the DNA strands covering the OGNPs. This effect was taken into account for each CFS run independently, once and before new addition of any OGNP to the system, randomizing which DNA ink sites formed well with a probability of Y_{ink}. This parameter effectively reduced the length of the chains formed in accordance with the experimental CFE data (see Figure S9 for complete yield study): non well-formed inks created regions in which the OGNPs could not attach. Y_{ink} was the only tunable, free, parameter of the simulation. All the rest were set according to experimental estimates.
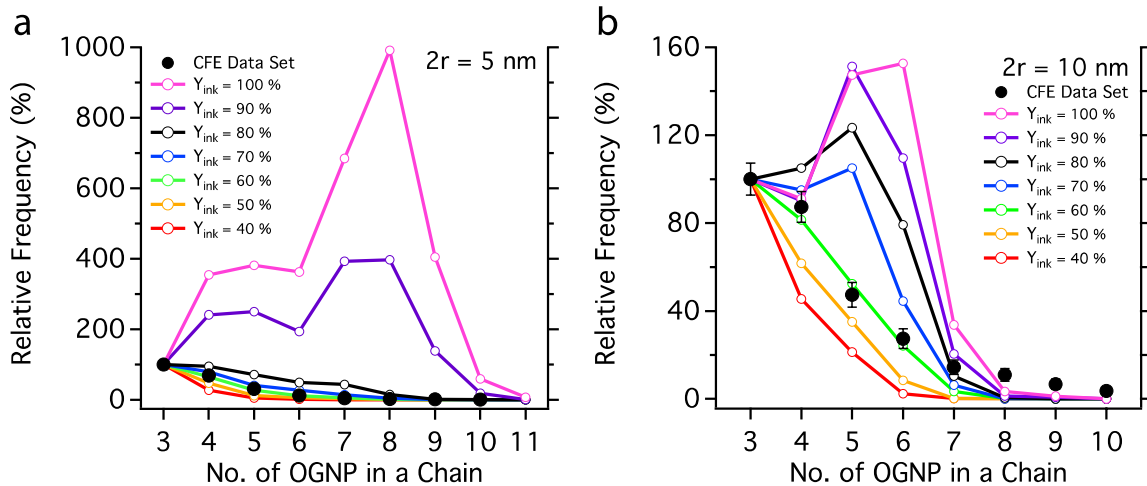

Figure S9. Complete yield analysis of DNA ink from CFS runs for OGNPs of 5 and 10 nm.

Convergence (i.e. computational stability and systematic uncertainty reduction) of this numerical method with respect to the problem size *(N, M)* —i.e. the number of OGNP added

and the number of CFS runs averaged —was studied before carrying out the simulations presented in the paper.

N accounted for the number of positions that could possibly be explored in one CFS run. The larger N value is, the more exhaustive the search. As the process is self-limiting, it was confirmed that N values as of 10000 allowed for exploring all possible arrangements in most configurations, leading to virtually equivalent results (see Figure S10 left panel).

From each ensemble of M equivalent CFS runs, statistics were extracted. To that end, the chains formed in each CFS run were identified and counted. Our SEM experiments showed that only the chains containing 3 or more nanoparticles were representative of the DNA template driven process (see main text). For this reason, chains of less than 3 OGNPs in length were discarded. During the counting process of the chains, only the longest chain in each CFS run was counted, and the rest were discarded. This is similar to the chain counting procedure used during the SEM image analysis: only chains containing close packing of aligned OGNPs were systematically counted as chain formation.
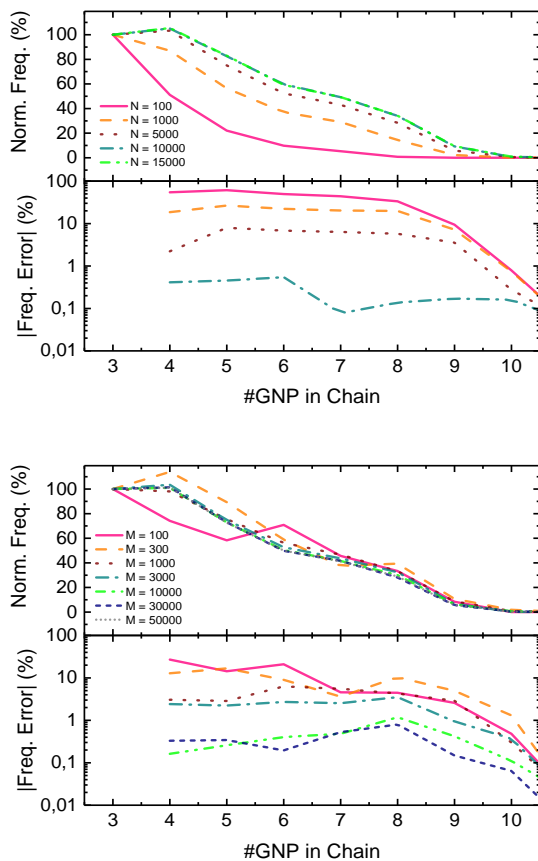
Figure S10. Model convergence analysis. (Left) As a function of the number of OGNP launched N in each CFS run. (Right) As a function of the number of CFS runs M averaged per simulation. Absolute simulation errors (i.e. |Freq. Error|) are calculated as the difference of each result with our best estimate (i.e. the most consuming simulation in each case: $N = 15000$, or $M = 50000$)

34
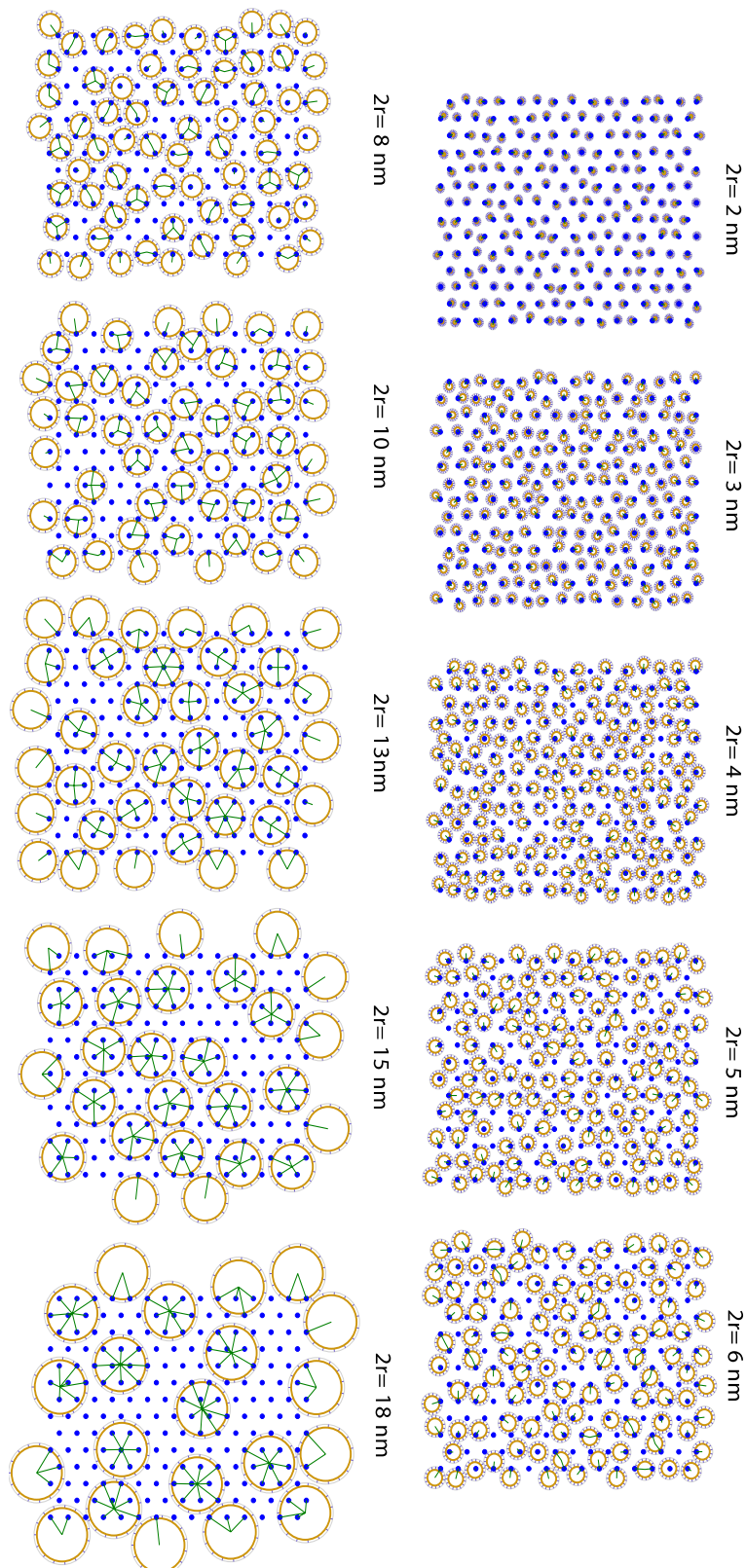
Figure S11. Analysis of effect of the OGNP diameter on the PFS runs. In these simulations were taken in account all DNA ink (all the staples) of the mesh, according to the tall rectangle DNA origami design. The Y_{ink} for all the Montecarlo simulations was of 100 %. The size of the gold nanoparticle used during is indicated for each simulation.
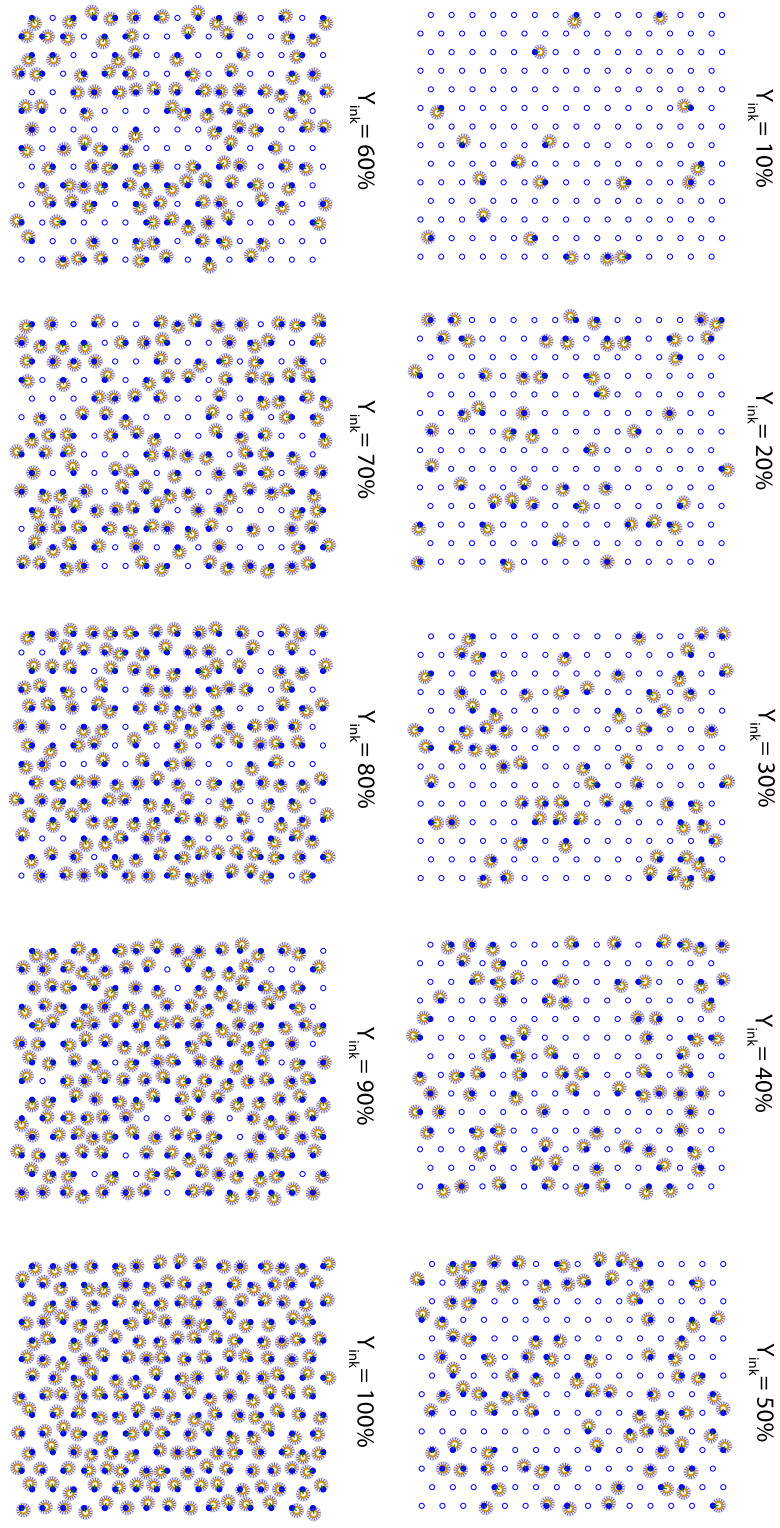
Figure S12. Analysis of effect of Y_{ink} during the PFS runs. In these experiments were taken in account all DNA ink (all the staples) of the mesh, according to the tall rectangle DNA origami design. The OGNP diameter used for all the Montecarlo simulations was of 2r = 3 nm. The Y_{ink} is indicated for each simulation result.

9. DNA Sequences

Table S1: Sequences (5'-3') of thiol-modified DNA ink staple strands, X corresponds to a disulfide modification: 5'-phosphate-O-$(CH_2)_6$-S-S-$(CH_2)_6$-OH.

t-5r16f-thiol	XTTTTTTTTTATATAATGGGGGCGCGAGCTGAAATTAACATC
t-5r16e-thiol	XTTTTTTTTTTTTCATTTCTGTAGCTCAACATGTTTAGAGAG
t-3r16f-thiol	XTTTTTTTTTTGCAACTAGGTCAATAACCTGTTTAGAATTAG
t-3r16e-thiol	XTTTTTTTTTTCGCAAATAAGTACGGTGTCTGGACCAGACCG
t-1r16f-thiol	XTTTTTTTTTTCCATATATTTAGTTTGACCATTAAGCATAAA
t-1r16e-thiol	XTTTTTTTTTCGAGTAGAACAGTTGATTCCCAATATTTAGGC
t1r16f-thiol	XTTTTTTTTTAGAGGCATACAACGCCAACATGTATCTGCGAA
t1r16e-thiol	XTTTTTTTTTCATATTTATTTCGAGCCAGTAATAAATCAATA
t3r16f-thiol	XTTTTTTTTTTAAAGTACCAGTAGGGCTTAATTGCTAAATTT
t3r16e-thiol	XTTTTTTTTTTACGCTCAACGACAAAAGGTAAAG TATCCCATC
t5r16f-thiol	XTTTTTTTTTCCAGACGACAAATTCTTACCAGTAGATAAATA
t5r16e-thiol	XTTTTTTTTTTGCGTTATACGACAATAAACAACATACAATAGA
t5r4e-thiol	XTTTTTTTTTTCGGCATTCCGCCGCCAGCATTGATGATATTC
t5r28e-thiol	XTTTTTTTTTTGAAATGGAAAACATCGCCATTAAACAGAGGTG

Table S2: Sequences (5'-3') of oligonucleotides complementary to the thiolated staple strands (bridge sequences). The underline sequence is the constant sequence that bridges the thiolated staple sequences to the gold nanoparticles by the DNA-CG sequence shown below.

t-5r16f-bridge	<u>CGAGTCATTGAGTCA</u>GATGTTAATTTCAGC
t-5r16e-bridge	<u>CGAGTCATTGAGTCA</u>CTCTCTAAACATGTT
t-3r16f-bridge	<u>CGAGTCATTGAGTCA</u>CTAATTCTAAACAGG
t-3r16e-bridge	<u>CGAGTCATTGAGTCA</u>CGGTCTGGTCCAGAC
t-1r16f-bridge	<u>CGAGTCATTGAGTCA</u>TTTATGCTTAATGGT
t-1r16e-bridge	<u>CGAGTCATTGAGTCA</u>GCCTAAATATTGGGA
t1r16f-bridge	<u>CGAGTCATTGAGTCA</u>TTCGCAGATACATGT
t1r16e-bridge	<u>CGAGTCATTGAGTCA</u>TATTGATTTATTACT
t3r16f-bridge	<u>CGAGTCATTGAGTCA</u>AAATTTAGCAATTAA
t3r16e-bridge	<u>CGAGTCATTGAGTCA</u>GATGGGATACTTTAC
t5r16f-bridge	<u>CGAGTCATTGAGTCA</u>TATTTATCTACTGGT
t5r16e-bridge	<u>CGAGTCATTGAGTCA</u>TCTATTGTATGTTGT
t5r4e-bridge	<u>CGAGTCATTGAGTCA</u>GAATATCATCAATGC
t5r28e-bridge	<u>CGAGTCATTGAGTCA</u>CACCTCTGTTTAATG

Sequence of thiolated oligonucleotide to link to gold nanoparticles

DNA-CG: 5'-<u>TGACTCAATGACTCG</u>TTTTTTTTTT-3'-phosphate-$(CH_2)_3$-SH

Table S3: List of the staple strands used to build the DNA origami.

t1r0g	AGGGTTGATATAAGTATAGCCCGGAATAGGTG
t1r2e	TAAGCGTCGGTAATAAGTTTTAACCCGTCGAG
t1r2f	AGTGTACTATACATGGCTTTTGATCTTTCCAG
t1r4e	AACCAGAGACCCTCAGAACCGCCACGTTCCAG
t1r4f	GAGCCGCCCCACCACCGGAACCGCTGCGCCGA
t1r6e	GACTTACGTAAAGGTCGCAACATACCGTCACC
t1r6f	AATCACCACCATTTGGGAATTAGACCAACCTA
t1r8e	TTATTACGTAAAGGTCGCAACATACCGTCACC
t1r8f	TACATACACAGTATGTTAGCAAACTGTACAGA
t1r10e	TGAACAAAGATAACCCACAAGAATAAGACTCC
t1r10f	ATCAGAGAGTCAGAGGGTAATTGAACCAGTCA
t1r12e	TATTTGCACGCTAACGAGCGTCTGAACACCC
t1r12f	TCTTACCAACCCAGCTACAATTTTAAAGAAGT
t1r14e	ATCGGGCTGACCAAGTACCGCACTCTTAGTTGC
t1r14f	GGTATTAATCTTTCCTTATCATTCATATCGCG
t1r16e	CATATTTATTTCGAGCCAGTAATAAATCAATA
t1r16f	AGAGGCATACAACGCCAACATGTATCTGCGAA
t1r18e	ACAAAGAAAATTTCATCTTCTGACAGAATCGC
t1r18f	TTTTAGTTCGCGAGAAAACTTTTTTTATGACC
t1r20e	AAATCAATCGTCGCTATTAATTAAATCGCAAG
t1r20f	CTGTAAATATATGTGAGTGAATAAAAAGGCTA
t1r22e	TTTAACGTTCGGGAGAAACAATAACAGTACAT
t1r22f	CTTTTACACAGATGAATATACAGTGCCATCAA
t1r24e	TTATTAATGAACAAAGAAACCACCTTTTCAGG
t1r24f	ATTTTGCGTTTAAAAGTTTGAGTACCGGCACC
t1r26e	CTAAAGCAAATCAATATCTGGTCACCCGAACG
t1r26f	AAACCCTCTCACCTTGCTGAACCTAGAGGATC
t1r28e	CTAAAAGCAAATCAATATCTGGTCACCCGAACG
t1r28f	GCGTAAGAAGATAGAACCCTTCTGAACGCGCG
t1r30e	GTTGTAGCCCTGAGTAGAAGAACTACTTCTG
t1r30f	ATCACTTGAATACTTCTTTGATTAGTTGTTCC
t1r32h	TACAGGGCGCGTACTATGGTTGCTAATTAACC
t3r0g	TGCTCAGTACCAGGCGGATAAGTGGGGGTCAG
t3r2e	GGAAAGCGGTAACAGTGCCCGTATCGGGGTTT
t3r2f	TGCCTTGACAGTCTCTGAATTTACCCCTCAGA
t3r4f	GCCACCACTCTTTTCATAATCAAATAGCAAGG
t3r6e	TTATTCATGTCACCAATGAAACCATTATTAGC
t3r6f	CCGGAAACTAAAGGTGAATTATCATAAAAGAA

t3r8f	ACGCAAAGAAGAACTGGCATGATTTGAGTTAA
t3r10e	GCGCATTAATAAGAGCAAGAAACAATAACGGA
t3r10f	GCCCAATAGACGGGAGAATTAACTTTCCAGAG
t3r12f	CCTAATTTAAGCCTTAAATCAAGAATCGAGAA
t3r14e	CTAATTTACCGTTTTTATTTTCATCTTGCGGG
t3r14f	CAAGCAAGCGAGCATGTAGAAACCAGAGAATA
t3r16f	TAAAGTACCAGTAGGGCTTAATTGCTAAATTT
t3r18e	TATGTAAAGAAATACCGACCGTGTTAAAGCCA
t3r18f	AATGGTTTTGCTGATGCAAATCCATTTTCCCT
t3r20f	TAGAATCCCCTTTTTTAATGGAAACGGATTCG
t3r22e	ACAGAAATCTTTGAATACCAAGTTAATTTCAT
t3r22f	CCTGATTGAAAGAAATTGCGTAGAAGAAGGAG
t3r24e	CGACAACTTCATCATATTCCTGATCACGTAAA
t3r24f	CGGAATTACGTATTAAATCCTTTGGTTGGCAA
t3r26e	GCCACGCTTTGAAAGGAATTGAGGAAACAATT
t3r26f	ATCAACAGGAGAGCCAGCAGCAAAATATTTTT
t3r28e	GTCACACGATTAGTCTTTAATGCGGCAACAGT
t3r28f	GAATGGCTACCAGTAATAAAAGGGCAAACTAT
t3r30e	GTAAAGACTGGTAATATCCAGAAATTCACCA
t3r30f	CGGCCTTGGTCTGTCCATCACGCATTGACGAG
t3r32h	CACGTATAACGTGCTTTCCTCGTTGCCACCGA
t5r0g	CCTCAAGAGAAGGATTAGGATTAGAAACAGTT
t5r2e	ACAAACAACTGCCTATTTCGGAACCTGAGACT
t5r4e	TCGGCATTCCGCCGCCAGCATTGATGATATTC
t5r4f	CACCAGAGTTCGGTCATAGCCCCCTCGATAGC
t5r6e	ATTGAGGGAATCAGTAGCGACAGACGTTTTCA
t5r8e	GAAGGAAAAATAGAAAATTCATATTTCAACCG
t5r8f	TCACA ATCCC GAGGA AACGC AATAA TGAAATA
t5r10e	CTTTACAGTATCTTACCGAAGCCCAGTTACCA
t5r12e	GAGGCGTTTCCCAATCCAAATAAGATAGCAGC
t5r12f	ATTATTTATTAGCGAACCTCCCGACGTAGGAA
t5r14e	TAAGTCCTGCGCCCAATAGCAAGCAAGAACGC
t5r16e	GCGTTATACGACAATAAACAACATACAATAGA
t5r16f	CCAGACGACAAATTCTTACCAGTAGATAAATA
t5r18e	TAACCTCCAATAAGAATAAACACCTATCATAT
t5r20e	AAAACAAACTGAGAAGAGTCAATATACCTTTT
t5r20f	TTAAGACGATTAATTACATTTAACACAAAATC
t5r22e	AACCTACCGCGAATTATTCATTTCACATCAAG
t5r22f	GCGCAGAGATATCAAAATTATTTGTATCAGAT
t5r24e	GGATTTAGTTCATCAATATAATCCAGGGTTAG
t5r24f	GATGGCAAAAGTATTAGACTTTACAAGGTTAT
t5r26e	AGGCGGTCTCTTTAGGAGCACTAAACATTTGA

40

t5r26f	CTAAAATAAGTATTAACACCGCCTCGAACTGA
t5r28e	GAAATGGAAAACATCGCCATTAAACAGAGGTG
t5r28f	TAGCCCTATTATTTACATTGGCAGCAATATTA
t5r30e	AGAAGTGTCATTGCAACAGGAAAAAATCGTCT
t5r30f	CCGCCAGCTTTTATAATCAGTGAGAGAATCAG
t5r32h	AGCGGGAGCTAAACAGGAGGCCGAGAATCCTG
t-1r0g	TATCACCGTACTCAGGAGGTTTAGATAGTTAG
t-1r2e	ACGTTAGTTCTAAAGTTTTGTCGTGATACAGG
t-1r2f	CGTAACGAAAATGAATTTTCTGTAGTGAATTT
t-1r4e	CAATGACAGCTTGATACCGATAGTCTCCCTCA
t-1r4f	CTTAAACAACAACCATCGCCCACGCGGGTAAA
t-1r6e	AAACGAAATGCCACTACGAAGGCAGCCAGCAA
t-1r6f	ATACGTAAGAGGCAAAAGAATACACTGACCAA
t-1r8e	CCAGGCGCGAGGACAGATGAACGGGTAGAAAA
t-1r8f	CTTTGAAAATAGGCTGGCTGACCTACCTTATG
t-1r10e	GGACGTTGAGAACTGGCTCATTATGCGCTAAT
t-1r10f	CGATTTTAGGAAGAAAAATCTACGGATAAAAA
t-1r12e	TTTGCCAGGCGAGAGGCTTTTGCAATCCTGAA
t-1r12f	CCAAAATAAGGGGGTAATAGTAAAAAAGATT
t-1r14e	TTTTAATTGCCCGAAAGACTTCAACAAGAACG
t-1r14f	AAGAGGAACGAGCTTCAAAGCGAAAGTTTCAT
t-1r16e	CGAGTAGAACAGTTGATTCCCAATATTTAGGC
t-1r16f	TCCATATATTTAGTTTGACCATTAAGCATAAA
t-1r18e	CTGTAATAGGTTGTACCAAAAACACAAATATA
t-1r18f	GCTAAATCCTTTTGCGGGAGAAGCCCGGAGAG
t-1r20e	TCAGGTCATTTTTGAGAGATCTACCCTTGCTT
t-1r20f	GGTAGCTATTGCCTGAGAGTCTGGTTAAATCA
t-1r22e	AAATAATTTTTAACCAATAGGAACAACAGTAC
t-1r22f	GCTCATTTCGCGTCTGGCCTTCCTGGCCTCAG
t-1r24e	GCTTCTGGCACTCCAGCCAGCTTTACATTATC
t-1r24f	GAAGATCGTGCCGGAAACCAGGCAGTGCCAAG
t-1r26e	CCCGGGTACCTGCAGGTCGACTCTCAAATATC
t-1r26f	CTTGCATGCCGAGCTCGAATTCGTCCTGTCGT
t-1r28e	GGGAGAGGCATTAATGAATCGGCCACCTGAAA
t-1r28f	GCCAGCTGCGGTTTGCGTATTGGGAATCAAAA
t-1r30e	AGTTTGGACGAGATAGGGTTGAGTGTAATAAC
t-1r30f	GAATAGCCACAAGAGTCCACTATTAAGCCGGC
t-1r32h	GAACGTGGCGAGAAAGGAAGGGAATGCGCCGC
t-3r0g	CCCTCAGAACCGCCACCCTCAGAAACAACGCC
t-3r2e	TGCTAAACTCCACAGACAGCCCTCTACCGCCA
t-3r4e	ATATATTCTCAGCTTGCTTTCGAGTGGGATTT
t-3r4f	TCGGTTTAGGTCGCTGAGGCTTGCAAAGACTT

t-3r6e	CTCATCTTGGAAGTTTCCATTAAACATAACCG
t-3r8e	AGTAATCTTCATAAGGGAACCGAACTAAAACA
t-3r8f	ACGGTCAATGACAAGAACCGGATATGGTTTAA
t-3r10e	ACGAACTATTAATCATTGTGAATTTCATCAAG
t-3r12e	ACTGGATATCGTTTACCAGACGACTTAATAAA
t-3r12f	CATAACCCGCGTCCAATACTGCGGTATTATAG
t-3r14e	GAAGCAAAAAAGCGGATTGCATCAATGTTTAG
t-3r16e	TCGCAAATAAGTACGGTGTCTGGACCAGACCG
t-3r16f	TGCAACTAGGTCAATAACCTGTTTAGAATTAG
t-3r18e	CAACGCAAAGCAATAAAGCCTCAGGATACATT
t-3r20e	AGAGAATCAGCTGATAAATTAATGCTTTATTT
t-3r20f	ACCGTTCTGATGAACGGTAATCGTAATATTTT
t-3r22e	CTTTCATCTCGCATTAAATTTTTGAGCAAACA
t-3r22f	GTTAAAATAACATTAAATGTGAGCATCTGCCA
t-3r24e	TTCGCCATGGACGACGACAGTATCGTAGCCAG
t-3r24f	GTTTGAGGTCAGGCTGCGCAACTGTTCCCAGT
t-3r26e	TCATAGCTTGTAAAACGACGGCCAAAGCGCCA
t-3r26f	CACGACGTGTTTCCTGTGTGAAATTTGCGCTC
t-3r28e	TGGTTTTTCTTTCCAGTCGGGAAAAATCATGG
t-3r28f	ACTGCCCGCTTTTCACCAGTGAGATGGTGGTT
t-3r30e	TGGACTCCGGCAAAATCCCTTATACGCCAGGG
t-3r30f	CCGAAATCAACGTCAAAGGGCGAAAAGGGAGC
t-3r32h	CCCCGATTTAGAGCTTGACGGGGAAAAGAACG
t-5r0g	CTCAGAGCCACCACCCTCATTTTCCGTAACAC
t-5r2e	GAGAATAGGTCACCAGTACAAACTCCGCCACC
t-5r2f	TGAGTTTCAAAGGAACAACTAAAGATCTCCAA
t-5r4f	AAAAAAGGCTTTTGCGGGATCGTCGGGTAGCA
t-5r6e	GCGAAACAAGAGGCTTTGAGGACTAGGGAGTT
t-5r6f	ACGGCTACAAGTACAACGGAGATTCGCGACCT
t-5r8f	GCTCCATGACGTAACAAAGCTGCTACACCAGA
t-5r10e	AAAGATTCTAAATTGGGCTTGAGATTCATTAC
t-5r10f	ACGAGTAGATCAGTTGAGATTTAGCGCCAAAA
t-5r12f	GGAATTACCATTGAATCCCCCTCACCATAAAT
t-5r14e	TACCTTTAAGGTCTTTACCCTGACAATCGTCA
t-5r14f	CAAAAATCATTGCTCCTTTTGATAATTGCTGA
t-5r16f	ATATAATGGGGGCGCGAGCTGAAATTAACATC
t-5r18e	TATATTTTCATACAGGCAAGGCAAAGCTATAT
t-5r18f	CAATAAATAAATGCAATGCCTGAGAAGGCCGG
t-5r20f	AGACAGTCTCATATGTACCCCGGTTTGTATAA
t-5r22e	ACCCGTCGTTAAATTGTAAACGTTAAAACTAG
t-5r22f	GCAAATATGATTCTCCGTGGGAACCGTTGGTG
t-5r24e	GGCGATCGCGCATCGTAACCGTGCGAGTAACA

t-5r24f	TAGATGGGGTGCGGGCCTCTTCGCGCAAGGCG
t-5r26e	GCTCACAAGGGTAACGCCAGGGTTTTGGGAAG
t-5r26f	ATTAAGTTTTCCACACAACATACGCCTAATGA
t-5r28e	AGCTGATTACTCACATTAATTGCGTGTTATCC
t-5r28f	GTGAGCTAGCCCTTCACCGCCTGGGGTTTGCC
t-5r30e	TATCAGGGCGAAAATCCTGTTTGACGGGCAAC
t-5r30f	CCAGCAGGCGATGGCCCACTACGTGAGGTGCC
t-5r32h	GTAAAGCACTAAATCGGAACCCTAAAACCGTC

10. References

[29]   T. A. Taton, *Curr Protoc Nucleic Acid Chem* **2002**, *Chapter 12*, Unit 12 2.

[30]   S. A. Claridge, H. W. Liang, S. R. Basu, J. M. Frechet, A. P. Alivisatos, *Nano Lett* **2008**, *8*, 1202.

[31]   J. Schindelin, I. Arganda-Carreras, E. Frise, V. Kaynig, M. Longair, T. Pietzsch, S. Preibisch, C. Rueden, S. Saalfeld, B. Schmid, J. Y. Tinevez, D. J. White, V. Hartenstein, K. Eliceiri, P. Tomancak, A. Cardona, *Nat Methods* **2012**, *9*, 676.

[32]   Z. Zhao, E. L. Jacovetty, Y. Liu, H. Yan, *Angew. Chem. Int. Ed. Engl.* **2011**, *50*, 2041.